Halide-Bridged Palladium(II) Dimers of Orthometalated (*S*)-(+)-*N*,*N*-Dimethyl-α-methylbenzylamine and (*S*)-(+)-*N*,*N*-Dimethyl[1-(2-naphthyl)ethyl]amine: Solution and Solid-State Structures and Reactions with 3,4-Dimethyl-1-phenylphosphole and Allyldiphenylphosphine

Nizamettin Gül and John H. Nelson*

Department of Chemistry/216, University of Nevada-Reno, Reno, Nevada 89557-0020

Received August 23, 1999

Activation thermodynamics for the cis ⇌ trans isomerization of the chloride-, bromide-, and iodide-bridged palladium(II) dimers of orthometalated (*S*)-(+)-*N*,*N*-dimethyl-α-methylbenzylamine (TMBA) and (*S*)-(+)-*N*,*N*-dimethyl[1-(2-naphthyl)-ethyl]amine (TMNA) have been determined by variable-temperature ^{1}H NMR spectroscopy. The chloride-bridged dimers are cleaved regioselectively by 3,4-dimethyl-1-phenylphosphole (DMPP) and allyldiphenylphosphine (ADPP) to form the mononuclear products {Pd($C_6H_4CH(Me)$)$NMe_2(R_3P)Cl$} and {Pd($C_{10}H_6CH(Me)$)$NMe_2(R_3P)Cl$} (R_3P = DMPP, ADPP), with the phosphine exclusively trans to nitrogen. The chloride-bridged dimers react with $NaPF_6$ or $AgClO_4$, DMPP, and CH_3CN to produce {Pd($C_6H_4CH(Me)$)NMe_2(DMPP)(CH_3CN)}X and {Pd($C_{10}H_6CH(Me)$)NMe_2(DMPP)(CH_3CN)}X (X = PF_6^-, ClO_4^-). They react with $NaPF_6$ or $AgClO_4$ and excess DMPP to form [Pd(DMPP)$_4$](X)$_2$ (X = PF_6^-, ClO_4^-). When X = PF_6^-, this complex undergoes two thermal [2+2] dimerizations of the coordinated DMPP ligands in the solid state to form {Pd(DMPP$_2$-[2+2])$_2$}$(PF_6)_2$. The complex {Pd($C_{10}H_6CH(Me)$)NMe_2(DMPP)Cl} reacts with $AgClO_4$ and ADPP at 75 °C to form an unusual chloride-bridged tetrapalladium(II) macrocycle that contains a novel tridentate ligand with bridging phosphide and terminal R_3P and C(−) donors. New complexes were characterized by elemental analyses, physical properties, infrared spectroscopy, polarimetry, and ^{1}H, ^{1}H{^{31}P}, ^{13}C{^{1}H}, and ^{31}P{^{1}H} NMR spectroscopy and in most cases by X-ray crystallography.

Introduction

Palladium(II) complexes containing orthometalated chiral amines such as **1a**−**3a** are useful reagents (1) for the resolution of chiral phosphines and arsines,[1] (2) for the determination of the optical purity of chiral phosphines by ^{31}P{^{1}H} NMR spectroscopy,[2] and (3) as templates for the asymmetric syntheses of conformationally rigid bidentate ligands derived from metal-promoted intramolecular [4+2] Diels−Alder cycloadditions of 3,4-dimethyl-1-phenylphosphole (DMPP) with a variety of dienophilic ligands.[3] Complexes **1a**−**3a** undergo facile bridge-splitting reactions with a variety of two-electron donor ligands to give mononuclear species.

Complex **3a** crystallizes as the cis isomer from either CH_2Cl_2 or $CHCl_3$ solutions, in which it undergoes a facile rearrangement into an approximately 4:3 ratio of cis and trans diastereomers. Concentration of these solutions, in both cases, affords the pure cis diastereomers[4] in a typical second-order asymmetric transforma-

(1) Wild, S. E. *Coord. Chem. Rev.* **1997**, *166*, 291.
(2) (a)Kyba, E. P.; Rines, S. P. *J. Org. Chem.* **1982**, *47*, 4800. (b) Nelson, J. H. *Coord. Chem. Rev.* **1995**, *139*, 245.
(3) (a) Leung, P.-H.; Loh, S. K.; Mok, K. F.; White, A. J. P.; Williams, D. J. *J. Chem. Soc., Chem. Commun.* **1996**, 591. (b) Aw, B. H.; Leung, P.-H.; White, A. J. P.; Williams, D. J. *Organometallics*, **1996**, *15*, 3640. (c) Selvaratnam, S.; Mok, K. F.; Leung, P.-H.; White, A. J. P.; Williams, D. J. *Inorg. Chem*, **1996**, *35*, 4798. (d) Leung, P.-H.; Loh, S. K.; Mok, K. F.; White, A. J. P.; Williams, D. J. *J. Chem. Soc., Dalton Trans.* **1996**, 4443. (e) Aw, B. H.; Hor, T. S. A.; Selvaratnam, S.; White, A. J. P.; Williams, D. J.; Rees, N. H.; McFarlane, W.; Leung, P.-H. *Inorg. Chem.* **1997**, *36*, 2138. (f) Leung, P.-H.; Selvaratnam, S.; Cheng, C. R.; Mok, K. F.; Rees, N. H.; McFarlane, W. *J. Chem. Soc., Chem. Commun.* **1997**, 751. (g) Liu, A. M.; Mok, K. F.; Leung, P.-H. *J. Chem. Soc., Chem. Commun.* **1997**, 239. (h) Leung. P.-H.; Siah, S. Y.; White, A. J. P.; Williams, D. J. *Chem. Soc., Dalton Trans.* **1998**, 893. (i) Song, Y.; Vittal, J. J.; Chan, S.-H.; Leung, P.-H. *Organometallics* **1999**, *18*, 650. (j) Gül, N.; Nelson, J. H. *Tetrahedron*, in press. (k) Lang, H.; Vittal, J. J.; Leung, P.-H. *J. Chem. Soc., Dalton Trans.* **1998**, 2109. (l) Leung, P.-H.; Liu, A.; Mok, K. F. *Tetrahedron: Asymmetry*, **1999**, *10*, 1309.

(4) Hockless, D. C. R.; Gugger, P. A.; Leung, P.-H.; Mayadunne, R. C.; Pabel, M.; Wild, S. B. *Tetrahedron*, **1997**, *53*, 4083.
(5) (a) Turner, E. E.; Harris, M. M. *Q. Rev.* **1947**, *1*, 299. (b) Jacques, J.; Collet, A.; Wilen, S. H. *Enantiomers, Racemates and Resolutions*; Wiley-Interscience: New York, 1981; pp 371−377.
(6) Hockless, D. C. R.; Gugger, P. A.; Wild, S. B. Unpublished work cited in ref 1.

10.1021/om990681a CCC: $19.00
Publication on Web 12/08/1999

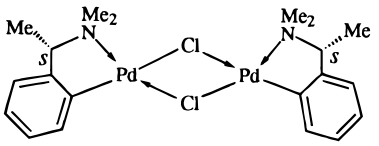

(*S,S*)-**1a**

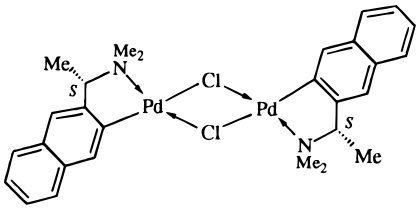

(*S,S*)-**2a**

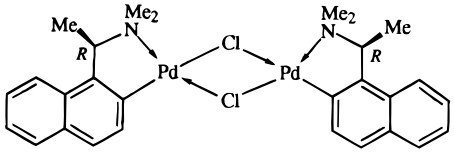

(*R,R*)-**3a**

tion.[5] Complex **1a** is said[1] to behave similarly, but no data have been reported.[6]

We have undertaken a detailed study of the solid-state structures and solution behavior of complexes **1a**, **2a**, and their bromide and iodide derivatives in order to relate this behavior to their relative utility as resolving agents for chiral phosphines and as templates for asymmetric syntheses of chiral bidentate ligands. Complex **1a** is a good resolving agent for triarylphosphines, whereas **2a** is a good resolving agent for mixed alkylarylphosphines.[7] Both **2a** and **3a** are good templates for asymmetric syntheses.[3] We have also studied the reactions of **1a** and **2a** with DMPP and ADPP because of the utility of the products for the asymmetric syntheses of chiral bidentate ligands.[3] The results of these studies are described herein.

Results and Discussion

A. Syntheses and Structures of 1a−c and 2a−c. Complexes **1a**[7] and **2a**[7] react with NaBr or NaI in acetone/water mixtures to readily form the crystalline air-stable bromide (**1b**, **2b**) and iodide (**1c**, **2c**) analogues (Scheme 1), respectively. The solid-state structures of **1b**, **1c**, **2a**, and **2b** were determined by X-ray crystallography (Figures 1 and 2). Crystallographic data are listed in Tables 1 and 2, and selected bond distances and angles are given in the figure captions. All four complexes crystallize as discrete molecular entities with no unusual intermolecular contacts. Complex **2a** crystallizes as a hydrate with two inequivalent molecules in the asymmetric unit, and **2b** crystallizes as a CH_2Cl_2 solvate.

Scheme 1

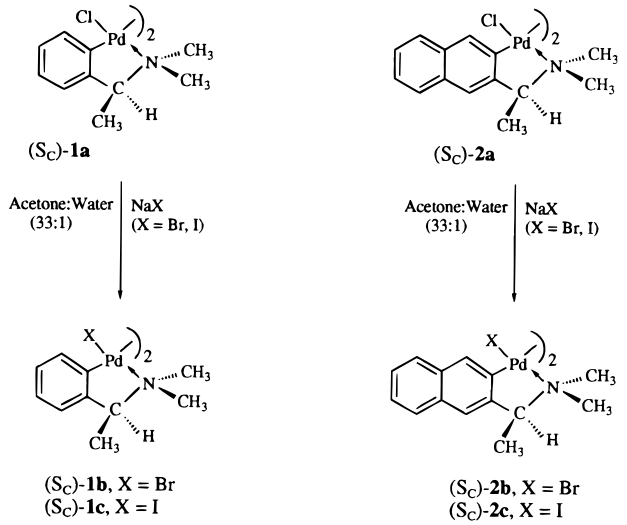

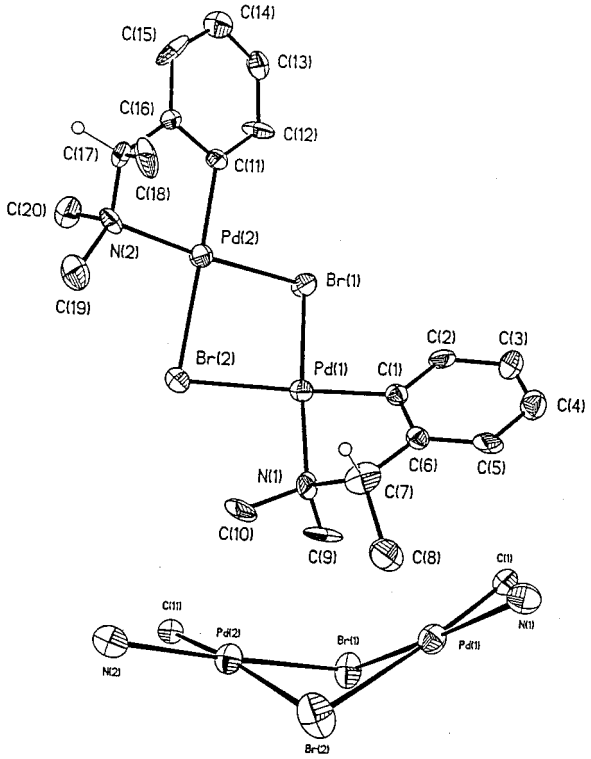

Figure 1. Structural drawings of **1b** showing the atom-numbering scheme (40% probability ellipsoids). Hydrogen atoms have an arbitrary radius of 0.1 Å. Selected bond distances (Å) and angles (deg): Pd(1)−C(1), 1.97(2); Pd(2)−C(11), 2.00(2); Pd(1)−N(1), 2.10(2); Pd(2)−N(2), 2.11(2); Pd(1)−Br(1), 2.466(2); Pd(2)−Br(1), 2.458(2); Pd(1)−Br(2), 2.584(2); Pd(2)−Br(2), 2.596(3); C(1)−Pd(1)−N(1), 81.5(7); C(11)−Pd(2)−N(2), 80.9(6); C(1)−Pd(1)−Br(1), 94.1(5); C(11)−Pd(2)−Br(1), 95.1(5); N(1)−Pd(1)−Br(2), 99.3(4); N(2)−Pd(2)−Br(2), 99.2(4); Br(1)−Pd(1)−Br(2), 84.98(8); Br(1)−Pd(2)−Br(2), 84.90(8). Selected bond distances (Å) and angles (deg) for **1c**: Pd(1)−C(1), 1.988(8); Pd(2)−C(11), 1.990(7); Pd(1)−N(1), 2.124(7); Pd(2)−N(2), 2.113(6); Pd(1)−I(1), 2.5959(7); Pd(2)−I(1), 2.5967(8); Pd(1)−I(2), 2.7402(8); Pd(2)−I(2), 2.7459(8); C(1)−Pd(1)−N(1), 81.5(3); C(11)−Pd(2)−N(2), 81.6(3); C(1)−Pd(1)−I(1), 95.7(2); C(11)−Pd(2)−I(1), 95.1(2); N(1)−Pd(1)−I(2), 95.7(2); N(2)−Pd(2)−I(2), 97.1(2); I(1)−Pd(1)−I(2), 87.08(2); I(1)−Pd(2)−I(2), 86.95(2).

The benzylamine complexes (**1b**, **1c**) have the cis geometry, whereas the naphthylamine complexes (**2a**, **2b**) have the trans geometry. Though X-ray quality crystals of **1a** and **2c** could not be obtained from a number of different solvents, it seems reasonable to assume that they would possess the cis and trans geometries exhibited by their other halide analogues.

(7) Tani, K.; Brown, L. D.; Ahmed, J.; Ibers, J. A.; Yokota, M.; Nakamura, A.; Otsuka, S. *J. Am. Chem. Soc.* **1997**, *99*, 77876.

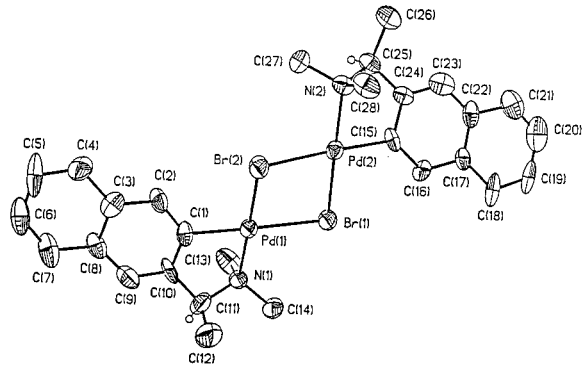

Figure 2. Structural drawing of **2b** showing the atom-numbering scheme (40% probability ellipsoids). Hydrogen atoms have an arbitrary radius of 0.1 Å. Selected bond distances (Å) and angles (deg): Pd(1)−C(1), 2.00(2); Pd(2)−C(15), 1.972(14); Pd(1)−N(1), 2.094(13); Pd(2)−N(2), 2.090(12); Pd(1)−Br(1), 2.590(2); Pd(2)−Br(1), 2.449(2); Pd(1)−Br(2), 2.450(2); Pd(2)−Br(2), 2.601(2); C(1)−Pd(1)−N(1), 80.8(7); C(15)−Pd(2)−N(2), 81.9(6); C(1)−Pd(1)−Br(2), 96.6(6); C(15)−Pd(1)−Br(1), 94.4(5); N(1)−Pd(1)−Br(1), 96.6(3); N(2)−Pd(2)−Br(2), 97.8(4); Br(1)−Pd(1)−Br(2), 86.46(7); Br(1)−Pd(2)−Br(2), 86.24(7). Selected bond distances (Å) and angles (deg) for **2a**: Pd(1)−C(1), 1.96(2); Pd(2)−C(15), 1.973(12); Pd(1)−N(1), 2.084(13); Pd(2)−N(2), 2.06(2); Pd(1)−Cl(1), 2.336(4); Pd(2)−Cl(1), 2.487(4); Pd(1)−Cl(2), 2.475(4); Pd(2)−Cl(2), 2.338(4); C(1)−Pd(1)−N(1), 80.3(6); C(15)−Pd(2)−N(2), 82.9(6); C(1)−Pd(1)−Cl(1), 94.9(5); C(15)−Pd(2)−Cl(2), 94.7(5); N(1)−Pd(1)−Cl(2), 98.8(4); N(2)−Pd(2)−Cl(1), 96.8(4); Cl(1)−Pd(1)−Cl(2), 86.21(14); Cl(1)−Pd(2)−Cl(2), 85.89(13).

Table 1. Crystallographic Data for 1b, 1c, and 2a

	1b	**1c**	**2a**
emp formula	$C_{20}H_{28}Br_2N_2Pd_2$	$C_{20}H_{28}I_2N_2Pd_2$	$C_{28}H_{32}Cl_2N_2Pd_2{\cdot}H_2O$
fw	669.06	763.04	696.26
cryst syst	orthorhombic	orthorhombic	monoclinic
a (Å)	8.3411(9)	10.1745(4)	6.6179(7)
b (Å)	9.665(12)	14.927(2)	12.924(2)
c (Å)	27.295(4)	15.480(2)	35.545(5)
α (deg)	90	90	90
β (deg)	90	90	89.995(6)
γ (deg)	90	90	90
V (Å^3)	2200.7(5)	2350.9(4)	3040.1(7)
Z	4	4	4[c]
space group	$P2_12_12_1$	$P2_12_12_1$	$P2_1$
ρ_{calcd} (g/cm^3)	2.019	2.156	1.521
μ (cm^{-1})	52.72	41.63	13.80
R1(*F*)[a] [*I* > 2σ(*I*)]	0.0625	0.0379	0.0509
wR2(F^2)[b]	0.1068	0.0789	0.1457
GOF	0.999	1.024	1.197
Flack param	0.05(3)	−0.06(4)	0.05(8)

[a] $R1(F) = \sum(||F_o| - |F_c||)/\sum(|F_o|)$. [b] $wR2(F^2) = \{\sum[w(F_o^2 - F_c^2)^2]/\sum[w(F_o^2)^2]\}^{1/2}$. [c] Two inequivalent molecules in the asymmetric unit.

The palladium(II) coordination geometries are planar for all four complexes, as the sums of the angles around palladium are all near 360°. All four complexes have butterfly structures with dihedral angles between the two palladium coordination planes of 24.7° (**1b**), 16.5° (**1c**), 17.4° (**2a**), and 16.9° (**2b**). This angle appears to decrease with increasing size of the ligands bound to palladium(II). For complex **3a**, because of an unfavorable interaction between the carbon-methyl group of the organometallic ring and H(8) of the naphthalenyl ring in the complex, the carbon-methyl group selectively adopts an axial disposition in a ring of *δ* conformation when the chiratropic carbon to which it is attached has the *R* absolute configuration.[4] For complexes **1b**, **2a**, and **2b** one carbon-methyl group is axial and the other is equatorial, but for **1c** both carbon-methyl groups are axial. Mercury complexes[8] of *N*,*N*-dimethyl[1-(2-naphthyl)ethyl]amine (TMNA) have equatorial carbon-methyl groups as do η^6-arene ruthenium(II) complexes of both TMNA[9,10] and *N*,*N*-dimethyl-α-methylbenzylamine (TMBA).[11,12] For the TMBA complexes the five-membered organometallic ring is generally flexible in solution and interconverts between two limiting conformations, but for the η^6-arene ruthenium(II) TMNA complexes[9,10] and for **3a**[4] the five-membered organometallic ring is generally rigid in solution.

Table 2. Crystallographic Data for 2b and 5

	2b	**5**
emp formula	$C_{28}H_{32}Br_2N_2Pd_2{\cdot}CH_2Cl_2$	$C_{25}H_{29}ClNPPd$
fw	854.10	516.31
cryst syst	orthorhombic	orthorhombic
a (Å)	6.6927(7)	8.2020(8)
b (Å)	12.9415(14)	16.0334(12)
c (Å)	36.059(4)	17.592(2)
α (deg)	90	90
β (deg)	90	90
γ (deg)	90	90
V (Å^3)	3123.2(6)	2313.4(4)
Z	4	4
space group	$P2_12_12_1$	$P2_12_12_1$
ρ_{calcd} (g/cm^3)	1.816	1.482
μ (cm^{-1})	39.02	9.98
R1(F)[a] [*I* > 2σ(*I*)]	0.0617	0.0483
wR2(F^2)[b]	0.1004	0.0927
GOF	1.000	0.999
Flack param	0.02(2)	−0.14(8)

[a] $R1(F) = \sum(||F_o| - |F_c||)/\sum(|F_o|)$. [b] $wR2(F^2) = \{\sum[w(F_o^2 - F_c^2)^2]/\sum[w(F_o^2)^2]\}^{1/2}$.

For all four complexes (**1b**, **1c**, **2a**, and **2b**) one of the Pd−X bonds is shorter (and presumably stronger) than the other. For the cis-isomers (**1b** and **1c**) this bond length difference may be ascribed to the different trans influences[13] of carbon and nitrogen donor ligands. However, the average Pd−X bond length difference for the cis-isomers (0.138 Å) is in fact slightly shorter than that (0.145 Å)for the trans-isomers (**2a** and **2b**), militating against this explanation. For **3a** the difference is 0.103 Å.[4] Evidently, independent of geometry, for complexes of this type, one Pd−X bond is inherently shorter than the other, and this may provide some insight into why these species are so labile in solution.

(8) Gül, N.; Nelson, J. H. *J. Mol. Struct.* **1999**, *475*, 121.
(9) Gül, N.; Nelson, J. H. *Organometallics* **1999**, *18*, 709.
(10) Gül, N.; Nelson, J. H. *Polyhedron* **1999**, *18*, 1835.
(11) (a) Attar, S.; Catalano, V. J.; Nelson, J. H. *Organometallics* **1996**, *15*, 2932. (b) Attar, S.; Nelson, J. H.; Fischer, J.; De Cian, A.; Sutter, J.-P.; Pfeffer, M. *Organometallics* **1995**, *14*, 4559. (c) Hansen, H. D.; Maitra, K.; Nelson, J. H. *Inorg. Chem.* **1999**, *38*, 2150.
(12) (a) Van der Schaaf, P. A.; Boersma, J.; Kooijman, H.; Speck, A. L.; Van Koten, G. *Organometallics* **1993**, *12*, 4334. (b) Alcock, N. W.; Hulmes, D. I.; Brown, J. M. *J. Chem. Soc., Chem. Commun.* **1995**, 395. (c) Jiang, Q.; Rüegger, H.; Venanzi, L. M. *J. Organomet. Chem.* **1995**, *488*, 233. The first two citations claim that equatorial carbon-methyl groups are rarely found in complexes of these types of ligands, whereas the third claims that they are found approximately 50% of the time for such rings.
(13) (a) Appleton, T. G.; Clark, H. C.; Manzer, L. E. *Coord. Chem. Rev.* **1973**, *10*, 335. (b) Gofman, M. M.; Nefedov, V. I. *Inorg. Chim. Acta* **1978**, *28*, 1.

Table 3. Activation Thermodynamics for the Cis ⇌ Trans Isomerization of Complexes 1a−c and 2a−c

complex	solvent	$\Delta G^{\ddagger}_{298}$ (±0.5 kcal mol^{-1})	$\Delta H^{\ddagger}$ (±0.5 kcal mol^{-1})	$\Delta S^{\ddagger}$ (±1 eu)
1a	$CDCl_3$	16.0	9.2	−22.9
	C_6D_6	15.6	5.3	−34.5
	toluene-d_8	15.5	5.6	−33.3
1b	$CDCl_3$	15.9	10.2	−19.4
	C_6D_6	15.3	5.6	−32.6
	toluene-d_8	15.2	4.9	−34.7
1c	$CDCl_3$	15.8	10.4	−18.2
	C_6D_6	15.1	5.2	−33.1
	toluene-d_8	15.4	5.9	−31.9
2a	$CDCl_3$	16.4	12.7	−12.5
	C_6D_6	15.7	3.2	−42.1
	toluene-d_8	16.2	4.2	−40.6
2b	$CDCl_3$	15.8	7.3	−28.4
	C_6D_6	15.5	4.6	−36.7
	toluene-d_8	15.6	3.7	−39.7
2c	$CDCl_3$	15.6	3.3	−41.1
	C_6D_6	15.2	4.7	−35.3
	toluene-d_8	15.3	6.3	−30.2

B. Solution Behavior of 1a−c and 2a−c. The 500 MHz ^{1}H and 125 MHz $^{13}C\{^1H\}$ NMR spectra of **1a−c** and **2a−c** in $CDCl_3$, C_6D_6, and toluene-d_8 all show the presence of two species in an approximately 1:1 ratio, as there are two resonances observed for each chemically inequivalent proton and carbon nucleus type. The ratios of the two species are temperature independent within experimental error between 20 °C and the coalescence temperature (50−80 °C depending upon the complex and the solvent), but the line widths increase and the chemical shift differences decrease, up to the coalescence point, with increasing temperature. The variable-temperature ^{1}H NMR spectra were thus treated as equally populated two-site exchange systems[14] to obtain exchange rates and from Eyring plots activation thermodynamics for the cis ⇌ trans isomerization processes (Table 3).

As can be seen from the data in Table 3, both $\Delta H^{\ddagger}$ and $\Delta S^{\ddagger}$ are solvent sensitive, with $\Delta H^{\ddagger}$ decreasing and $\Delta S^{\ddagger}$ increasing in magnitude with increasing solvent donor ability.[15] Because $\Delta H^{\ddagger}$ is small and positive and $\Delta S^{\ddagger}$ is large and negative, the isomerization is most likely a solvent-assisted associative process involving pentacoordinate palladium(II) transition states.

The ^{1}H NMR spectrum of a 1:1 mixture of **2a** and **2b** in $CDCl_3$ at 25 °C exhibits six NCH_3 resonances (δ 2.97, 2.94, 2.91, 2.75, 2.70, and 2.65 ppm) in a 2:1.6:1:1.6:2:1 ratio. None of these chemical shifts correspond to those of **2a** or **2b** in $CDCl_3$. Thus, three new species are present in this solution that we suggest are the mixed Cl/Br-bridged species **A**, **B**, and **C**, with the ratio **A** (1):**B** (1.6):**C** (2), respectively.

Wild and co-workers reported[4] that (*R**,*S**)-*trans*-**3a** selectively crystallized from a $CDCl_3$ solution of an equimolar mixture of (*R*,*R*)-*cis*-**3a** and (*S*,*S*)-*cis*-**3a**. Four species are present in this solution, viz., *cis*- and *trans*-(*R**,*R**)-(±)- and (*R**,*S**)-**3a**. These authors proposed that isomerization of **3a** involved the intermediacy of a highly reactive and undetected solvento species **D**. Our data are consistent with this same type of intermediate for the isomerizations of all these complexes.

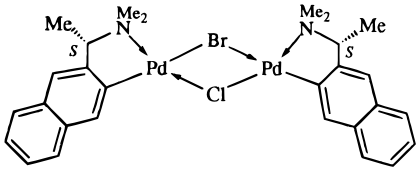

A

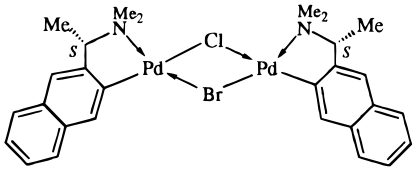

B

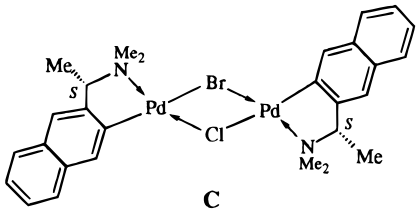

C

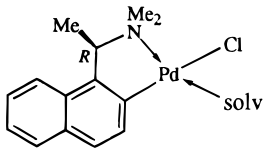

D

The ^{1}H and $^{13}C\{^1H\}$ NMR spectra of **1a−c** and **2a−c** in CD_3CN solutions at 25 °C all show only one resonance for each chemically inequivalent nucleus type, except for the presence of two CHD_2CN resonances (one broad and unresolved and one sharp five-line multiplet). The line widths of all the ^{1}H resonances and the chemical shift differences of the two CHD_2CN resonances all decrease with increasing temperature, consistent with exchange equilibria between free and coordinated CHD_2CN (eq 1).

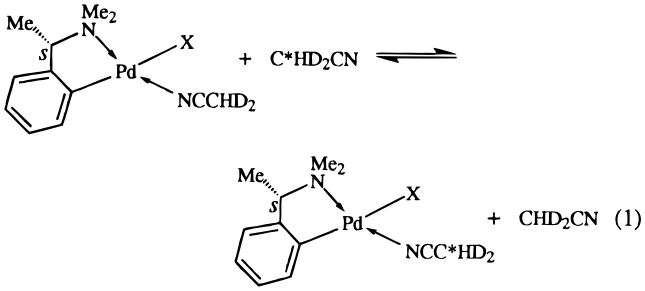

Thus, CD_3CN completely cleaves the dimers (**1a−c** and **2a−c**), but upon evaporation of CD_3CN these dimers are reformed. Similar equilibria were not observed for **3a**, suggesting that **1a** and **2a** are more labile than **3a**.

C. Reactions of 1a and 2a with DMPP and ADPP. DMPP and ADPP react with **1a** and **2a** in CH_2Cl_2 at ambient temperature to afford **4−7** (reaction 2) in high yields. All these complexes are air-stable crystalline solids.

(14) Sandstorm, J. *Dynamic NMR Spectroscopy*; Academic: New York, 1982.

(15) Gutmann, V. *The Donor−Acceptor Approach to Molecular Interactions*; Plenum: New York, 1978.

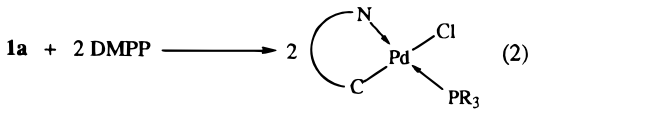

C N	PR_3
4 (*S*)-TMBA	DMPP
5 (*S*)-TMBA	ADPP
6 (*S*)-TMNA	DMPP
7 (*S*)-TMNA	ADPP

Complex **6** has been previously reported,[3j] and complex **4** has been used as a reagent in the asymmetric synthesis of a chiral diphosphine,[3k] but no characterization data have been reported for **4**. The $^{31}P\{^1H\}$ NMR spectrum of each complex shows only one singlet resonance. The ^1H and $^{13}C\{^1H\}$ NCH_3 resonances all exhibit $^4J(PH)$ and $^3J(PC)$ couplings of 2−5 Hz. Thus, these four complexes all form exclusively with the phosphorus donor ligands trans to nitrogen. The crystal structure of **6** has been described,[3j] and that of **5** is shown in Figure 3. Crystallographic data are given in Tables 4 and 5, and selected bond distances and angles are listed in the figure caption. Both **6** and **7** crystallize with two inequivalent molecules in the asymmetric unit. For both **6** and **7** one molecule has the carbon-methyl group in an axial position and the other molecule has the carbon-methyl group in an equatorial position. For **5** the carbon-methyl group is in an equatorial position. The palladium(II) coordination geometry is planar in each complex, as the sums of the angles around palladium are all near 360°. The metrical parameters of **5** and **7** are very similar, in concert with our previous conclusion[9] that TMBA and TMNA have essentially the same donor abilities. For all three complexes the phosphine is trans to nitrogen, and this gives rise to a lengthening of the Pd−N bond in **7** (2.163(3) Å) compared to those in the precursor **2a** (2.072(13) Å, av). The Pd−P bond in **6** (2.219(6) Å) is slightly shorter than that in **7** (2.2642(12) Å), suggesting that DMPP is a slightly better donor than ADPP. This is also reflected by the comparative Pd−N bond lengths for **6** (2.20(2) Å) and **7** (2.163(3) Å).

Complex **4** reacts with $AgNO_3$ in CH_3CN solution to form AgCl and **8**, as colorless crystals, that contains a monodentate nitrate as shown by infrared spectroscopy (ν_{NO} 1450, 1282, and 1019 cm^{-1}) and X-ray crystallography (Figure 4). Crystallographic data are given in Table 4, and selected bond distances and angles are given in the figure caption. The Pd−P (2.232(2) Å) and Pd−O (2.160(5) Å) bond distances are comparable to those found[16] for *cis*-$(DMPP)_2Pd(NO_3)_2$ (2.2455 Å, av and 2.111 Å, av, respectively). The palladium(II) coordination geometry is planar with the phosphole trans to the amine nitrogen, and the NO_3^- plane is inclined at a 70.1° angle to the coordination plane. The carbon-methyl group is axial.

In an attempt to prepare $[(TMBA)Pd(DMPP)_2]PF_6$ and $[(TMNA)Pd(DMPP)_2]PF_6$ in order to study the palladium-promoted dimerization of DMPP[17] in a chiral environment, **1a** and **2a** were each reacted with 5 molar equiv of DMPP in CH_2Cl_2 in the presence of $NaPF_6$ at ambient temperature. Surprisingly, $[(DMPP)_4Pd](PF_6)_2$, **9** (Scheme 2), was a major product of these reactions. After isolation of **9** from the reaction mixtures, the residues were crystallized from an CH_3CN/acetone/ether mixture to afford $[(TMBA)Pd(DMPP)(CH_3CN)]PF_6$ (**10**) and $[(TMNA)Pd(DMPP)(CH_3CN)]PF_6$ (**11**). Finally, TMBA and TMNA were recovered from the residues after crystallization of **10** and **11**. Complexes **10** and **11** were also prepared by reactions of **1a** and **2a** with 2 molar equiv of DMPP in CH_3CN solutions containing

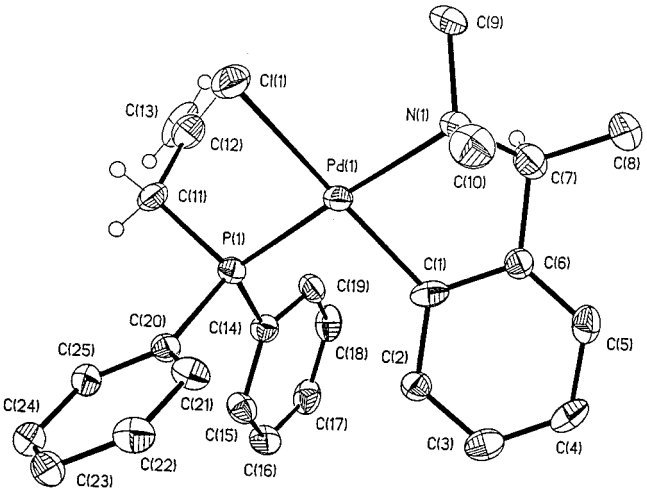

Figure 3. Structural drawing of **5** showing the atom-numbering scheme (30% probability ellipsoids). Hydrogen atoms have an arbitrary radius of 0.1 Å. Selected bond distances (Å) and angles (deg): Pd(1)−C(1), 2.006(8); Pd(1)−N(1), 2.154(7); Pd(1)−P(1), 2.248(2); Pd(1)−Cl(1), 2.409(2); C(12)−C(13), 1.267(13); C(1)−Pd(1)−N(1), 81.3(3); N(1)−Pd(1)−Cl(1), 93.06(18); Cl(1)−Pd(1)−P(1), 90.91(8); P(1)−Pd(1)−C(1), 95.5(2). Selected bond distances (Å) and angles (deg) for **7**: Pd(1)−C(1), 2.004(4); Pd(1)−N(1), 2.163(3); Pd(1)−P(1), 2.2642(12); Pd(1)−Cl(1), 2.4056(14); C(16)−C(17), 1.290(7); C(1)−Pd(1)−N(1), 81.18(14); N(1)−Pd(1)−Cl(1), 93.26(9); Cl(1)−Pd(1)−P(1), 89.87(5); P(1)−Pd(1)−C(1), 95.84(12).

Table 4. Crystallographic Data for 7, 8, and 9

	7	**8**	**9**
emp formula	$C_{29}H_{31}ClNPPd$	$C_{22}H_{27}N_2O_3PPd$	$C_{48}H_{52}F_{12}P_6Pd$
fw	566.37	504.83	1149.12
cryst syst	triclinic	orthorhombic	triclinic
a (Å)	8.497(3)	13.3194(13)	10.9360(12)
b (Å)	12.436(5)	14.9466(12)	11.039(2)
c (Å)	12.584(13)	22.594(3)	11.7822(13)
α (deg)	83.09(3)	90	75.054(8)
β (deg)	84.25(3)	90	66.928(8)
γ (deg)	85.85(3)	90	78.266(10)
V ($Å^3$)	1311.0(8)	4497.9(8)	1256.0(3)
Z	2[c]	8[c]	1
space group	*P*1	$P2_12_12_1$	$P\bar{1}$
ρ_{calcd} (g/cm^3)	1.435	1.491	1.519
μ (cm^{-1})	8.88	9.21	6.39
R1(F)[a] [$I > 2\sigma(I)$]	0.0228	0.0402	0.0561
wR2(F^2)[b]	0.0582	0.0789	0.1252
GOF	1.004	1.011	1.087
Flack param	−0.03(2)	−0.02(4)	NA

[a] $R1(F) = \sum(||F_o| - |F_c||)/\sum(|F_o|)$. [b] $wR2(F^2) = \{\sum[w(F_o^2 - F_c^2)^2]/\sum[w(F_o^2)^2]\}^{1/2}$. [c] Two inequivalent molecules in the asymmetric unit.

(16) Redwine, K. D.; Wilson, W. L.; Moses, D. G.; Catalano, V. J.; Nelson, J. H. *Inorg. Chem.*, submitted for publication.

(17) Wilson, W. L.; Fischer, J.; Wasylishen, R. E.; Eichele, K.; Catalano, V. J.; Frederick, J. H.; Nelson, J. H. *Inorg. Chem.* **1996**, *35*, 1486.

Table 5. Crystallographic Data for 10, 11a, and 13

	10	11a	13
emp formula	$C_{24}H_{30}F_6N_2P_2Pd$	$C_{28}H_{32}ClN_2O_4PPd$	$C_{56}H_{59}Cl_4P_4Pd_4$
fw	628.84	633.38	1437.32
cryst syst	monoclinic	orthorhombic	triclinic
a (Å)	11.146(2)	8.2103(8)	11.689(1)
b (Å)	8.4375(15)	10.7349(12)	11.823(1)
c (Å)	30.023(5)	33.147(4)	12.377(1)
α (deg)	90	90	110.98(1)
β (deg)	99.120(15)	90	114.16(1)
γ (deg)	90	90	92.77(1)
V (Å^3)	2787.9(8)	2921.5(5)	1418.6(2)
Z	2[c]	4	1
space group	$P2_1$	$P2_12_12_1$	$P\bar{1}$
ρ_{calcd} (g/cm^3)	1.498	1.440	1.682
μ (cm^{-1})	8.35	8.16	15.86
R1(F)[a] $[I > 2\sigma(I)]$	0.0363	0.0377	0.0411
wR2(F^2)[b]	0.1014	0.0802	0.0953
GOF	1.432	1.043	0.999
Flack param	0.03(6)	−0.08(4)	−0.01(4)

[a] $R1(F) = \Sigma(||F_o| - |F_c||)/\Sigma(|F_o|)$. [b] $wR_2(F^2) = \{\Sigma[w(F_o^2 - F_c^2)^2]/\Sigma[w(F_o^2)^2]\}^{1/2}$. [c] Two inequivalent molecules in the asymmetric unit.

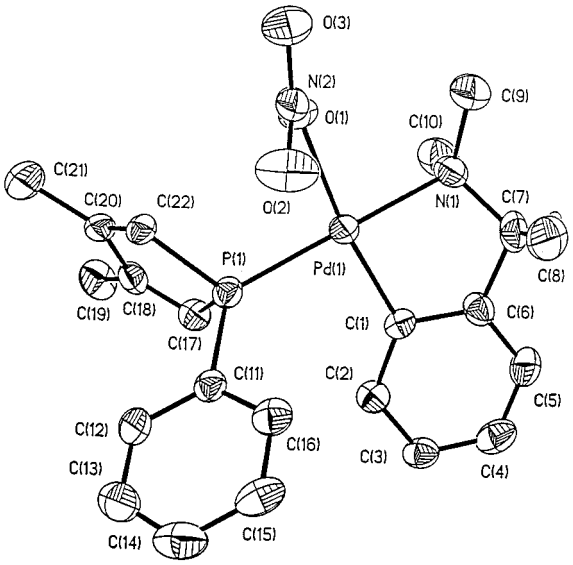

Figure 4. Structural drawings of **8** showing the atom-numbering scheme (40% probability ellipsoids). Selected bond distances (Å) and angles (deg): Pd(1)−C(1), 2.007(6); Pd(1)−N(1), 2.154(6); Pd(1)−P(1), 2.232(2); Pd(1)−O(1), 2.160(5); N(2)−O(1), 1.270(8); N(2)−O(2), 1.242(8); N(2)−O(3), 1.242(7); C(1)−Pd(1)−N(1), 82.1(3); N(1)−Pd(1)−O(1), 89.9(2); O(1)−Pd(1)−P(1), 94.29(5); O(1)−N(2)−O(2), 120.7(7); O(2)−N(2)−O(3), 121.3(8); O(3)−N(2)−O(1), 117.9(7).

$NaPF_6$. Similar reactions were observed (Scheme 3) between **4** or **6**, $AgClO_4$, and DMPP to afford the analogous perchlorate salts of **9**, **10**, and **11**.

Complexes **9**, **10**, and **11** were characterized spectroscopically (see the Experimental Section) and by X-ray crystallography (Figures 5 and 6). Crystallographic data are given in Tables 5 and 6, and selected bond distances and angles are listed in the figure captions. The metrical parameters for **10** and **11** are similar, as TMBA and TMNA have essentially the same donor abilities. For both complexes the palladium(II) coordination geometries are planar and the phosphole is trans to the amine nitrogen. Complex **10** crystallizes with two inequivalent molecules in the asymmetric unit. The carbon-methyl groups are axial for both molecules of **10**

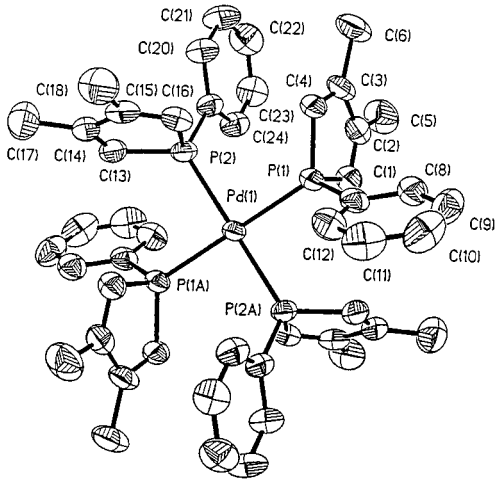

Figure 5. Structural drawing of the cation of **9** showing the atom-numbering scheme (40% probability ellipsoids). Selected bond distances (Å) and angles (deg): Pd(1)−P(1), 2.3461(14); Pd(1)−P(2), 2.3407(14); P(1)−Pd(1)−P(2), 89.45(5); P(1)−Pd(1)−P(2a), 90.55(5).

Scheme 2

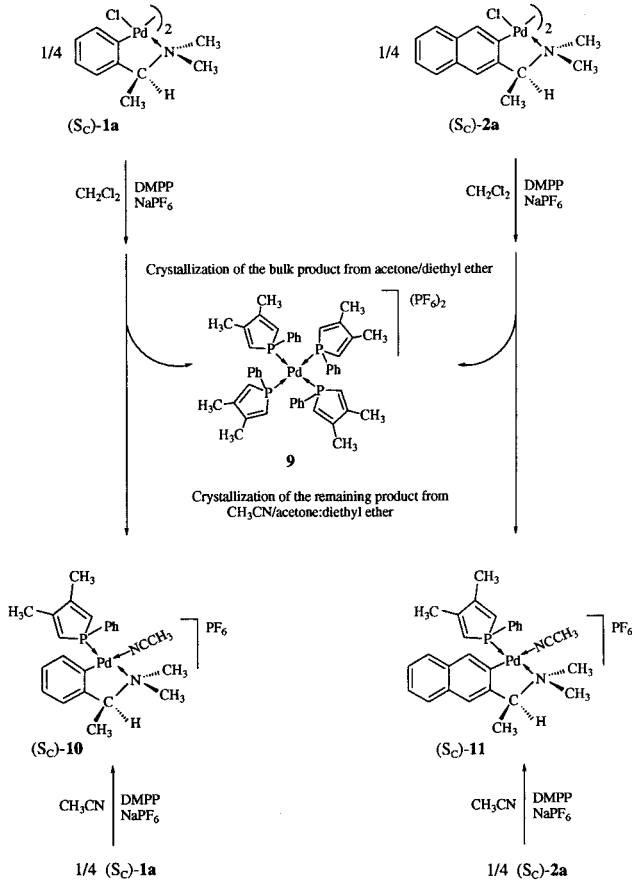

as well as for **11**. The coordination geometry of **9** is planar, with the palladium atom located on a crystallographic inversion center. The Pd−P distances in **9** (Pd(1)−P(1), 2.3461(14) Å, Pd(1)−P(2), 2.3407(14) Å) are very similar to those reported[18] for the structurally similar *meso*-[Pd(3,3′,4,4′-tetramethyl-1,1′-diphenyl-2,2′-biphosphole)]$(BF_4)_2$ complex [(biphos)$_2$-Pd]$(BF_4)_2$ (Pd−

(18) (a) Kojima, T.; Saeki, K.; Ono, K.; Ohba, M.; Matsuda, Y. *J. Chem. Soc., Chem. Commun.* **1997**, 1679. (b) Gouygou, M.; Tissot, D.; Daran, J.-C.; Balavoine, C. G. A. *Organometallics* **1997**, *16*, 1008.

Scheme 3

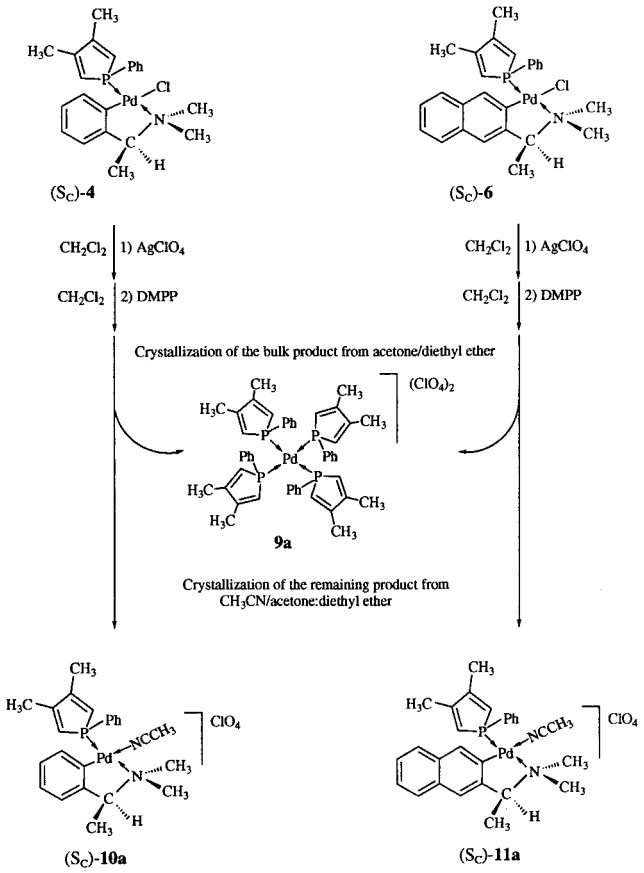

P, 2.338(3) Å, av). But the P−Pd−P bond angles in this complex, which are 84.51(5)° within the chelate ring and 95.49(5)° between the chelating biphospholes, are different from those in **9** (89.45(5)° and 90.55(5)°) because **9** contains four monodentate phospholes.

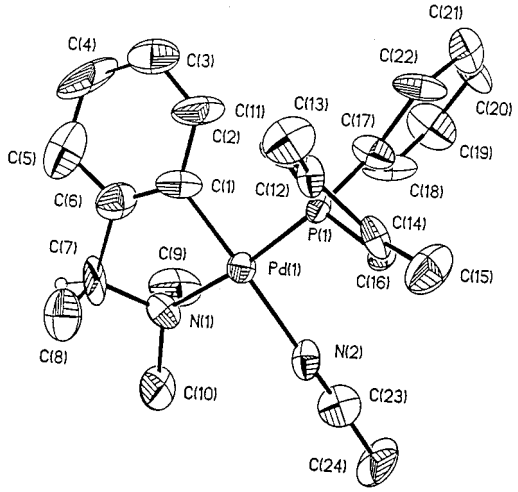

Figure 6. Structural drawing of the cation of **10** showing the atom-numbering scheme (40% probability ellipsoids). Hydrogen atoms have an arbitrary radius of 0.1 Å. Selected bond distances (Å) and angles (deg): Pd(1)−C(1), 1.991(11); Pd(1)−P(1), 2.256(3); Pd(1)−N(2), 2.135(8); Pd(1)−N(1), 2.095(9); N(2)−C(23), 1.149(13); C(1)−Pd(1)−P(1), 90.2(3); P(1)−Pd(1)−N(2), 95.8(2); N(2)−Pd(1)−N(1), 92.6(4); N(1)−Pd(1)−C(1), 81.9(4). Selected bond distances (Å) and angles (deg) for **11a**: Pd(1)−C(1), 1.988(5); Pd(2)−P(1), 2.2576(16); Pd(1)−N(2), 2.124(5); Pd(1)−N(1), 2.151(5); N(2)−C(27), 1.115(7); C(1)−Pd(1)−P(1), 90.96(17); P(1)−Pd(1)−N(2), 93.16(14); N(2)−Pd(1)−N(1), 95.23(18); N(1)−Pd(1)−C(1), 81.2(2).

Table 6. Crystallographic Data for 12 and (prophos)$PdCl_2$

	12	(prophos)$PdCl_2$
emp formula	$C_{48}H_{52}F_{12}P_6Pd\cdot 2C_3H_6O$	$C_{27}H_{26}Cl_2P_2Pd\cdot H_2O\cdot CH_2Cl_2$
fw	1256.47	690.64
cryst syst	triclinic	monoclinic
a (Å)	10.1129(18)	12.437(2)
b (Å)	11.9067(10)	15.809(2)
c (Å)	13.5945(17)	15.447(2)
α (deg)	93.697(9)	90
β (deg)	111.296(12)	104.704(1)
γ (deg)	103.476(14)	90
V (Å$^{3)}$	1462.9(3)	2937.8(8)
Z	1	4
space group	$P\bar{1}$	$P2_1/c$
ρ_{calcd} (g/cm^3)	1.436	1.562
μ (cm^{-1})	5.58	11.25
R1(F)[a] $[I > 2\sigma(I)]$	0.0863	0.0754
wR2($F2$)[b]	0.1754	0.1613
GOF	1.009	1.058

[a] $R1(F) = \Sigma(||F_o| - |F_c||)/\Sigma(|F_o|)$. [b] $wR2(F^2) = \{\Sigma[w(F_o^2 - F_c^2)^2]/\Sigma[w(F_o^2)^2]\}^{1/2}$.

The structural similarities of **9** and the biphosphole complex suggested to us that **9** might undergo a thermal palladium-promoted topotactic dimerization of adjacent phospholes in the solid state, similar to what we have reported for *cis*-$(DMPP)_2PdCl_2$[17] and *cis*-$(DMPP)_2PtCl_2$.[19] Indeed, heating solid **9** for 1 week at 145 °C in a sealed ampule gave rise to two [2+2] dimerizations of adjacent phospholes (reaction 3) to produce **12** in approximately 50% conversion.

$$[(DMPP)_4Pd](PF_6)_2 \xrightarrow{145\ ^\circ C} \underset{\mathbf{12}}{\left[\left(\begin{array}{c}\text{Ph}\\ \text{P}\end{array}\right)_2 \text{Pd}\right](PF_6)_2} \qquad (3)$$

9

Complex **12** was characterized spectroscopically (see Experimental Section). Notably, the $^{31}P\{^1H\}$ chemical shift for **12** (δ 89.80 ppm) occurs considerably downfield of those for **9** (21.96 ppm), *cis*-$(DMPP)_2PdCl_2$ (26.36 ppm), or $[(biphos)_2Pd](BF_4)_2$ (33.82 ppm).[18b] Complex **12** was also characterized by X-ray crystallography (Figure 7). Crystallographic data are given in Table 6, and selected bond distances and angles are listed in the figure caption. This complex crystallizes as an acetone solvate with disordered PF_6 ions. The palladium(II) coordination geometry is planar with the palladium atom located on a crystallographic inversion center. The space groups for **9** and **12** are both $P\bar{1}$, and the unit cell volume for **12** (1462.9 Å^3) is larger than that for **9** (1256.0(3) Å^3). Thus, the [2+2] dimerizations bring about an expansion in the crystal lattice, which mostly involves a lengthening of the *c*-axis. The four-membered ring in **12** is not square and the C(4)−C(6) bond length (1.643(13) Å) is much longer than the C(11)−C(12) bond length (1.378(14) Å), showing that there is considerable

(19) Wilson, W. L.; Rahn, J. A.; Alcock, N. W.; Fischer, J.; Frederick, J. H.; Nelson, J. H. *Inorg. Chem.* **1994**, *33*, 109.

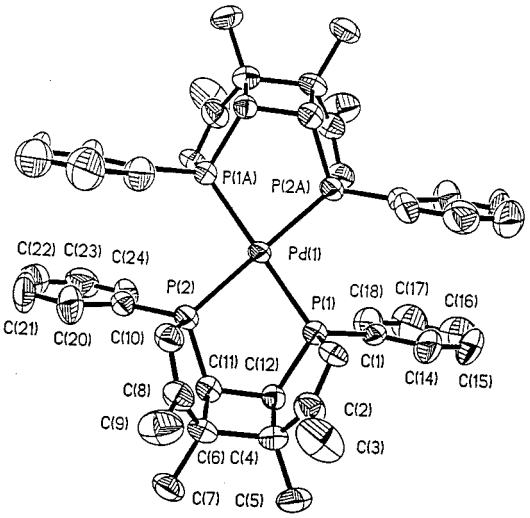

Figure 7. Structural drawing of the cation of **12** showing the atom-numbering scheme (40% probability ellipsoids). Selected bond distances (Å) and angles (deg): Pd(1)−P(1), 2.306(2); Pd(1)−P(2), 2.320(2); C(1)−C(2), 1.359(13); C(8)−C(10), 1.322(12); C(11)−C(12), 1.563(12); C(12)−C(4), 1.551(12); C(4)−C(16), 1.643(13); P(1)−Pd(1)−P(2), 83.35(8); P(1a)−Pd(1)−P(2), 96.65(8).

ring strain. This strain may lead to ring opening and conversion of the [2+2]-phosphole dimer into the [4+2]-phosphole dimer.[17,19] In this case none of the [4+2] dimer was isolated from the reaction.

Mathey and co-workers have well established the existence of an equilibrium between 1*H*-phospholes and 2*H*-phospholes at elevated temperature.[20] We have

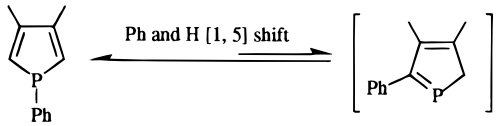

shown that the 2*H*-phosphole is more reactive than the 1*H*-phosphole and reacts with dienophiles such as ADPP to form 1-phosphanorbornenes[21] such as **E**. In an

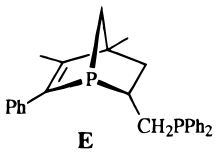

E

attempt at an asymmetric synthesis of **E**, complex **6** was reacted with $AgClO_4$ and ADPP in $ClCH_2CH_2Cl$ at 75 °C. Instead of **E**, the unusual red complex **13** was a major product of this reaction (Scheme 4). The structure of this complex was determined by X-ray crystallography (Figure 8). Crystallographic data are given in Table 5, and selected bond distances and angles are listed in the figure caption.

This complex may have been formed by the following sequence of events. ADPP and $AgClO_4$ somehow displaced TMNA from **6**. Then the free amine caused isomerization of coordinated ADPP to *trans*-propenyl-

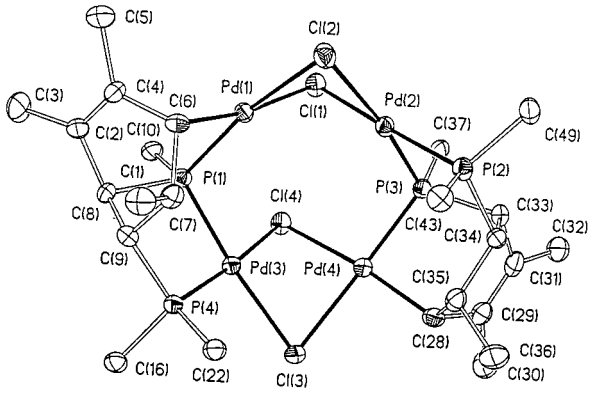

Figure 8. Structural drawing of the cation of **13** showing the atom-numbering scheme (40% probability ellipsoids). Phenyl groups have been omitted for clarity. Selected bond distances (Å) and angles (deg): Pd(1)−P(1), 2.231(3); Pd(1)−C(16), 2.078(10); Pd(1)−Cl(1), 2.489(3); Pd(1)−Cl(2), 2.458(3); Pd(1)−Pd(2), 3.0161(13); Pd(2)−Cl(1), 2.389(3); Pd(2)−Cl(2), 2.481(3); Pd(2)−P(2), 2.244(3); Pd(2)−P(3), 2.237(3); Pd(4)−P(3), 2.225(3); Pd(4)−C(28), 2.076(12); Pd(4)−Cl(3), 2.456(3); Pd(4)−Cl(4), 2.487(3); Pd(3)−Cl(4), 2.385(5); Pd(3)−Cl(3), 2.472(3); Pd(3)−P(4), 2.249(3); Pd(3)−P(1), 2.244(3); Pd(3)−Pd(4), 2.9945(13); P(1)−Pd(1)−C(6), 84.4(3); C(6)−Pd(1)−Cl(2), 91.6(3); Cl(2)−Pd(1)−Cl(1), 83.45(9); Cl(1)−Pd(1)−P(1), 101.87(10); Cl(1)−Pd(2)−Cl(2), 85.07(11); Cl(2)−Pd(2)−P(2), 99.89(10); P(2)−Pd(2)−P(3), 83.90(11); P(3)−Pd(2)−Cl(1), 91.46(10); P(3)−Pd(4)−C(28), 84.9(3); C(28)−Pd(4)−Cl(3), 91.4(3); Cl(3)−Pd(4)−Cl(4), 83.41(10); Cl(4)−Pd(4)−P(3), 101.51(10); Cl(4)−Pd(3)−P(1), 91.13(11); P(1)−Pd(3)−P(4), 84.72(11); P(4)−Pd(3)−Cl(3), 99.05(10); Cl(3)−Pd(3)−Cl(4), 85.21(10).

Scheme 4

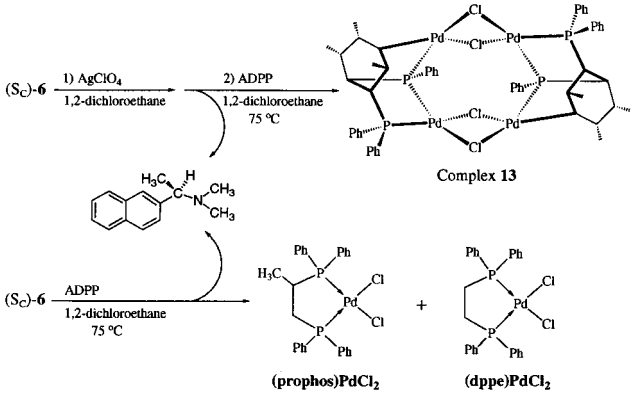

diphenylphosphine (*trans*-$CH_3CH{=}CHPPh_2$). This type of base-promoted isomerization of allylphosphines has been previously observed.[22] Then, an intramolecular [4+2] cycloaddition reaction afforded **F**. Insertion of $PdCl_2$ into the P(1)−C(1) bond of **F** finally gave rise to **13**. Insertions of this type as well as species such as **13**

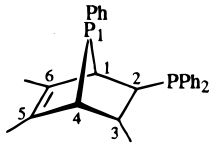

F

(20) (a) Mathey, F. *Chem. Rev.* **1988**, *88*, 429, and references therein. (b) Holland, S.; Jeanjean, M.; Mathey, F. *Angew. Chem., Int. Ed. Engl.* **1997**, *36*, 98.

(21) Maitra, K.; Catalano, V. J.; Nelson, J. H. *J. Am. Chem. Soc.* **1997**, *119*, 12560.

(22) (a) Mathey, F.; Muller, G. *Tetrahedron* **1972**, *27*, 5645. (b) Horner, L.; Ertel, I.; Ruprecht, H.-D.; Bélovský, O. *Chem. Ber.* **1970**, *103*, 1582.

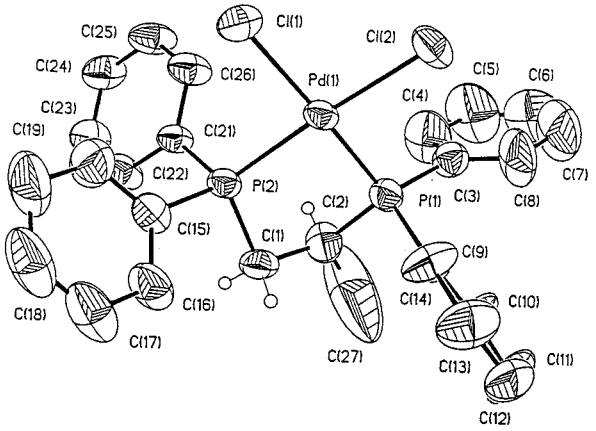

Figure 9. Structural drawing of (prophos)$PdCl_2$ showing the atom-numbering scheme (40% probability ellipsoids). Hydrogen atoms have an arbitrary radius of 0.1 Å. Selected bond distances (Å) and angles (deg): Pd(1)−P(1), 2.230(3); Pd(1)−P(2), 2.247(3); Pd(1)−Cl(1), 2.359(3); Pd(1)−Cl(2), 2.354(3); P(1)−Pd(1)−P(2), 86.13(10); P(1)−Pd(1)−Cl(2), 89.70(11); P(2)−Pd(1)−Cl(1), 90.98(10); Cl(2)−Pd(1)−Cl(1), 93.23(11).

are unprecedented. Complex **13** contains two bridging phosphides whose ^{31}P chemical shift (δ 221.92 ppm) occurs in the expected region.[23] The other phosphine resonance (δ 42.49 ppm) occurs in the region expected for a coordinated phosphine in a five-membered chelate ring.[24] The value of $^2J(PP) = 7.9$ Hz is characteristic of two cis-oriented phosphorus nuclei. Because of limited solubility, a $^{13}C\{^1H\}$ NMR spectrum could not be obtained and the ^1H NMR spectrum has a low signal-to-noise ratio.

The Pd(2) and Pd(3) centers are planar, but the Pd(1) and Pd(4) centers are distorted slightly from planarity. Each of the latter has a large P−Pd−Cl bond angle (101.87(10)° and 101.51(10)°) compared to the P−Pd−Cl bond angles around Pd(2) (91.46(10)°) and Pd(3) (91.13(11)°). The Pd(1,2) and Pd(3,4) moieties are hinged at the bridging chlorides, forming two butterfly species that are joined at each end by the tridentate P_2C donor ligands to form a large $Pd_4Cl_2P_2$-containing eight-membered ring. All the Pd−P bond lengths are similar, but two of the Pd−Cl bond lengths, namely, Pd(3)−Cl(4) (2.385(5) Å) and Pd(2)−Cl(1) (2.389(3) Å) are shorter than the other six Pd−Cl bond lengths (2.474 Å, av). The two Pd−C bond lengths are equal and in the expected range (2.077 Å, av). The C(2)−C(4) (1.326(16) Å) and C(29)−C(31) (1.331(17) Å) bond lengths are typical for carbon−carbon double bonds.

Reaction of **6** with ADPP in $ClCH_2CH_2Cl$ at 75 °C afforded unidentified products together with (dppe)$PdCl_2$[25] and *rac*-(prophos)$PdCl_2$.[26] Both these complexes were characterized by ^1H, $^{13}C\{^1H\}$, and $^{31}P\{^1H\}$ NMR spectroscopy. The ^{31}P chemical shifts are comparable to the literature values. The structure of (prophos)$PdCl_2$ was confirmed by X-ray crystallography (Figure 9). Crystallographic data are given in Table 6, and selected bond distances and angles are listed in the figure caption. The complex crystallizes with CH_2Cl_2 and H_2O in the crystal lattice. The palladium(II) coordination geometry is planar, and the two Pd−P and Pd−Cl bond lengths are essentially equal. The metrical parameters are very similar to those reported[27] for (dppe)$PdCl_2$.

Experimental Section

A. Reagents and Physical Measurements. All reagents were reagent grade and were used as received from commercial sources (Aldrich, Fischer Scientific, or Organometallics for ADPP). (S_C)-TMBA was a gift of HEXEL corporation. Silica gel for column chromatography (grade 200−300 mesh) was obtained from Natland International Corporation. DMPP[28] was prepared by the literature method. Elemental analyses were performed by Galbraith Laboratories, Knoxville, TN. Melting points were determined on a Mel-Temp apparatus and are uncorrected. FT-IR spectra were recorded as Nujol mulls on CsI windows for the far-IR region (30−710 cm^{-1}) and as thin films on KBr windows for the mid-IR region (400−4000 cm^{-1}) on a Perkin-Elmer BX-spectrometer (abbreviations: shp = sharp, sh = shoulder, st = strong, w = weak, b = broad). Optical rotations were measured on a Perkin-Elmer model 141 polarimeter. ^1H, $^1H\{^{31}P\}$, $^{13}C\{^1H\}$, and $^{31}P\{^1H\}$ NMR spectra were recorded at 499.8, 499.8, 125.7, and 202.3 MHz, respectively, on a Varian Unity-plus 500 FT-NMR spectrometer. Proton and carbon chemical shifts are relative to internal Me_4Si or solvent resonances, and phosphorus chemical shifts are relative to external 85% H_3PO_4 (aq) with positive values being downfield of the respective reference.

B. Synthesis. (*S*)-(+)-Bis(*μ*-chloro)bis[*N*,*N*-dimethyl-α-(2-naphthyl)ethylamine-*C*,*N*]dipalladium [(S_C)-2a]. Enantiomerically pure palladium complex (S_C)-**2a** was prepared from (*S*)-(−)-*N*,*N*-dimethyl-α-(2-naphthyl)ethylamine, TMNA,[8] and lithium tetrachloropalladate(II) in the presence of triethylamine as described in our previous report.[3j] ^1H NMR (499.8

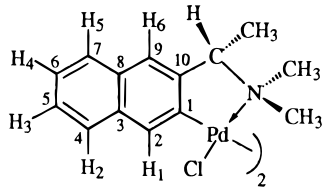

MHz, $CDCl_3$, 25 °C) *cis*-isomer: δ 7.79 (d, $^3J(H_2H_3) = 7.5$ Hz, 1H, H_2), 7.69 (d, $^3J(H_5H_6) = 6.5$ Hz, 1H, H_5), 7.68 (s, 1H, H_1), 7.35 (m, 2H, H_3, H_4), 7.25 (s, 1H, H_6), 4.03 (q, $^3J(HH) = 6.5$ Hz, 1H, CH), 2.96 (s, 3H, NCH_3), 2.70 (s, 3H, NCH_3), 1.66 (d, $^3J(HH) = 6.5$ Hz, 3H, CCH_3). *trans*-isomer: δ 7.72 (d, $^3J(H_2H_3) = 7.5$ Hz, 1H, H_2), 7.69 (d, $^3J(H_5H_6) = 6.5$ Hz, 1H, H_5), 7.59 (s, 1H, H_1), 7.35 (m, 2H, H_3, H_4), 7.22 (s, 1H, H_6), 4.00 (q, $^3J(HH) = 6.5$ Hz, 1H, CH), 2.92 (s, 3H, NCH_3), 2.65 (s, 3H, NCH_3), 1.64 (d, $^3J(HH) = 6.5$ Hz, 3H, CCH_3). Assignments for cis- and trans-isomers are arbitrary. $^{13}C\{^1H\}$ NMR (125.7 MHz, $CDCl_3$, 25 °C) *cis*-isomer: δ 150.85 (C_1), 141.17 (C_{10}), 131.65 (C_3), 131.56 (C_8), 131.34 (C_2), 127.21 (C_4), 127.11 (C_7), 125.15 (C_5), 124.50 (C_6), 120.14 (C_9), 74.77 (CH), 52.18 (NCH_3), 47.08 (NCH_3), 18.08 (CCH_3). *trans*-isomer: δ 150.74 (C_1), 140.99 (C_{10}), 131.59 (C_3), 131.56 (C_8), 130.86 (C_2), 127.11 (C_4), 127.11 (C_7), 125.10 (C_5), 124.50 (C_6), 120.14 (C_9), 74.57 (CH), 51.91 (NCH_3), 46.74 (NCH_3), 18.02 (CCH_3). The ^{13}C NMR assignments were made with the aid of APT and $^{13}C/^1H$ HETCOR experiments.

(*S*)-(+)-Bis(*μ*-chloro)bis[*N*,*N*-dimethyl-α-(phenyl)-ethylamine-*C*,*N*]dipalladium [(S_C)-1a]. Complex (S_C)-**1a**[7] was prepared similarly from Li_2PdCl_4 (0.015 mol), (*S*)-(−)-*N*,*N*-

(23) Carly, A. J.; MacLaughlin, S. A.; Nucciarone, D. In *Phosphorus-31 NMR Spectroscopy in Stereochemical Analysis*; Quin, L. D., Verkade, J. G., Eds.; VCH: Deerfield Beach, FL, 1987; pp 559−619.
(24) Garrou, P. E. *Chem. Rev.* **1981**, *81*, 229.
(25) Sanger, A. R. *J. Chem. Soc., Dalton Trans.* **1977**, 1971.
(26) Morandini, F.; Consiglio, G.; Piccolo, O. *Inorg. Chim. Acta* **1982**, *57*, 15.
(27) Steffan, W.-L.; Palenik, G. J. *Inorg. Chem.* **1976**, *15*, 2432.
(28) Bregue, A.; Mathey, F.; Savignac, P. *Synthesis* **1981**, 983.

dimethyl-α-(phenyl)ethylamine, TMBA (0.015 mol), and triethylamine (0.015 mol) as a pale yellow solid: mp 185−187 °C (blackens at 180 °C); $[\alpha]_D$ +101.6° (*c* 0.5, CH_2Cl_2); 3.26 g (75% yield). Anal. Calcd for $C_{20}H_{28}Cl_2N_2Pd_2$: C, 41.42; H, 4.83; Cl, 12.23. Found: C, 41.31; H, 4.72; Cl, 12.15. IR (CsI): ν_{Pd-Cl} 303 cm^{-1} (shp, st) and 260 cm^{-1} (shp, st). ^1H NMR (499.8 MHz,

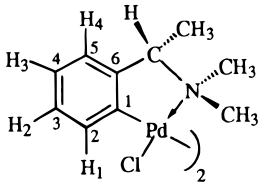

$CDCl_3$, 25 °C) *cis*-isomer: δ 7.20 (dd, $^3J(H_1H_2)$ = 7.5 Hz, $^4J(H_1H_3)$ = 1.0 Hz, 1H, H_1), 6.97 (apparent td, $^3J(H_1H_2)$ = $^3J(H_2H_3)$ = 7.5 Hz, $^4J(H_2H_4)$ = 1.0 Hz, 1H, H_2), 6.87 (apparent td, $^3J(H_2H_3)$ = $^3J(H_3H_4)$ = 7.5 Hz, $^4J(H_1H_3)$ = 1.0 Hz, 1H, H_3), 6.78 (dd, $^3J(H_3H_4)$ = 7.5 Hz, $^4J(H_2H_4)$ = 1.0 Hz, 1H, H_4), 3.89 (q, $^3J(HH)$ = 7.0 Hz, 1H, CH), 2.93 (s, 3H, NCH_3), 2.67 (s, 3H, NCH_3), 1.58 (d, $^3J(HH)$ = 7.0 Hz, 3H, CCH_3). trans-isomer: δ 7.16 (dd, $^3J(H_1H_2)$ = 7.5 Hz, $^4J(H_1H_3)$ = 1.0 Hz, 1H, H_1), 6.97 (apparent td, $^3J(H_2H_3)$ = $^3J(H_1H_2)$ = 7.5 Hz, $^4J(H_2H_4)$ = 1.0 Hz, 1H, H_2), 6.87 (apparent td, $^3J(H_2H_3)$ = $^3J(H_3H_4)$ = 7.5 Hz, $^4J(H_1H_3)$ = 1.0 Hz, 1H, H_3), 6.78 (dd, $^3J(H_3H_4)$ = 7.5 Hz, $^4J(H_2H_4)$ = 1.0 Hz, 1H, H_4), 3.87 (q, $^3J(HH)$ = 7.0 Hz, 1H, CH), 2.91 (s, 3H, NCH_3), 2.64 (s, 3H, NCH_3), 1.58 (d, $^3J(HH)$ = 7.0 Hz, 3H, CCH_3). Assignments for cis- and trans-isomers are arbitrary. $^{13}C\{^1H\}$ NMR (125.7 MHz, $CDCl_3$, 25 °C) *cis*-isomer: δ 152.29 (C_1), 143.39 (C_6), 133.33 (C_2), 125.22 (C_5), 124.62 (C_4), 121.95 (C_3), 75.29 (CH), 52.43 (NCH_3), 47.21 (NCH_3), 18.73 (CCH_3). trans-isomer: δ 152.12 (C_1), 143.37 (C_6), 132.82 (C_2), 125.22 (C_5), 124.62 (C_4), 121.95 (C_3), 75.16 (CH), 52.09 (NCH_3), 46.82 (NCH_3), 18.51 (CCH_3).

Synthesis and Characterization of (*S*)-(+)-Bis(*μ*-X)bis[L-*C*,*N*]dipalladium ([(*S*$_C$)-2b], X = Br, L = TMNA; [(*S*$_C$)-2c], X = I, L = TMNA; [(*S*$_C$)-1b], X = Br, L = TMBA; [(*S*$_C$)-1c], X = I, L = TMBA). Enantiomerically pure bromide and iodide analogues of the cyclopalladated complexes (*S*$_C$)-**1a** and (*S*$_C$)-**2a** were prepared by the same general method, i.e., the metathetic reactions depicted in Scheme 1. Reaction mixtures were not air sensitive, and no precautions were taken to exclude air. The reaction time for the Br^- reaction was 5 h longer than that of the I^- reaction. The following preparation of (*S*$_C$)-**2b** is representative.

(*S*$_C$)-2b. To a stirred solution of (*S*$_C$)-**2a** 0.8 g (1.18 mmol) in acetone (50 mL) was added a solution containing 0.365 g (3.54 mmol) of NaBr in water (1.5 mL). The resulting yellow solution was stirred at ambient temperature for 8 h, after which the solvent was removed under reduced pressure. The yellow-colored solid residue was dissolved in CH_2Cl_2 and filtered through a layer of $MgSO_4$ to remove NaCl, unreacted NaBr, and water. The pale yellow filtrate was taken to dryness on a rotary evaporator. The resulting solid was recrystallized from CH_2Cl_2/hexane to give (S$_C$)-**2b** as deep yellow prisms: mp 178−180 °C (blackens at 175 °C); $[\alpha]_D$ +42° (*c* 0.5, CH_2Cl_2); 0.82 g (81.7% yield). Anal. Calcd for $C_{28}H_{32}Br_2N_2Pd_2$: C, 43.74; H, 4.16; Br, 20.78. Found: C, 43.81; H, 4.09; Br, 20.67. IR (CsI): ν_{Pd-Br} 250 cm^{-1} (shp, w).

(*S*$_C$)-2c: mp 172−174 °C (blackens at 168 °C); $[\alpha]_D$ +159° (*c* 0.5, CH_2Cl_2); 0.80 g (78.5% yield). Anal. Calcd for $C_{28}H_{32}I_2N_2Pd_2$: C, 38.97; H, 3.71; I, 29.41. Found: C, 38.79; H, 3.55; I, 29.28. IR (CsI): ν_{Pd-I} 218 cm^{-1} (shp, w).

(*S*$_C$)-1b: mp 176−178 °C (blackens at 175 °C); $[\alpha]_D$ +122° (*c* 0.5, CH_2Cl_2); 0.60 g (75% yield). Anal. Calcd for $C_{20}H_{28}Br_2N_2Pd_2$: C, 35.91; H, 4.19; Br, 23.89. Found: C, 35.82; H, 4.03; Br, 23.76. IR (CsI): ν_{Pd-Br} 231 cm^{-1} (shp, w).

(*S*$_C$)-1c: mp 165−167 °C (blackens at 160 °C); $[\alpha]_D$ +148.6° (*c* 0.5, CH_2Cl_2); 0.65 g (72.5% yield). Anal. Calcd for $C_{20}H_{28}I_2N_2Pd_2$: C, 31.49; H, 3.67; I, 33.27. Found: 31.34; H, 3.50; I, 33.19. IR (CsI): ν_{Pd-I} 207 cm^{-1} (shp, w).

Synthesis and Characterization of (*S*$_C$)-4, (*S*$_C$)-5, (*S*$_C$)-6, and (*S*$_C$)-7. These complexes were all prepared by the same general method, i.e., cleavage of the dimers (*S*$_C$)-**1a** or (*S*$_C$)-**2a** by DMPP or ADPP. Reaction mixtures were air sensitive, and the reactions were performed under a dry nitrogen atmosphere. The following preparation of (*S*$_C$)-**7** is representative.

(*S*$_C$)-7. To 2.0 g (2.94 mmol) of the palladium dimer (*S*$_C$)-**2a** in 100 mL of CH_2Cl_2 under a nitrogen atmosphere was added 1.35 mL (6.18 mmol) of allyldiphenylphosphine (ADPP) via syringe. Upon addition of the phosphine, a transparent yellow solution formed. This solution was stirred magnetically for 10 h at ambient temperature. The solution was reduced in volume to ca. 5 mL via rotary evaporation, and *n*-hexane was added to precipitate the product as a pale yellow solid. The precipitate was isolated by filtration, washed with several small portions of a hexane−ether (1:1) mixture, and air-dried. The solid was recrystallized from $CHCl_3$/acetone/hexanes−ether (1:1) to afford pale yellow prisms: mp 191−193 °C; $[\alpha]_D$ +26.8° (*c* 0.5, CH_2Cl_2); 3.11 g (93.4% yield). Anal. Calcd for $C_{29}H_{31}ClNPPd$: C, 61.52; H, 5.48; Cl, 6.26. Found: C, 61.41; H, 5.36; Cl, 6.17. IR (CsI): ν_{Pd-Cl} 291 cm^{-1} (shp, st). $^{31}P\{^1H\}$ NMR (202.3 MHz,

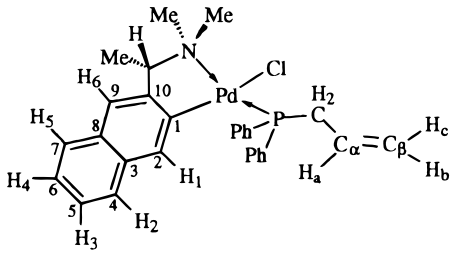

$CDCl_3$, 25 °C): δ 31.62 (s, 1P, ADPP). ^1H NMR (499.8 MHz, $CDCl_3$, 25 °C): δ 7.93 (m, 2H, H_o), 7.59 (dd, $^3J(H_2H_3)$ = 8.0 Hz, $^4J(H_2H_4)$ = 1.5 Hz, 1H, H_2), 7.46 (m, 3H, $H_{m,p}$), 7.38 (s, 1H, H_6), 7.37 (m, 2H, H_o), 7.32 (m, 3H, H_m, H_p), 7.24 (ddd, $^3J(H_2H_3)$ = 8.0 Hz, $^3J(H_3H_4)$ = 7.0 Hz, $^4J(H_3H_5)$ = 1.5 Hz, 1H, H_3), 7.15 (ddd, $^3J(H_4H_5)$ = 8.0 Hz, $^3J(H_3H_4)$ = 7.0 Hz, $^4J(H_2H_4)$ = 1.5 Hz, 1H, H_4), 6.96 (dd, $^3J(H_4H_5)$ = 8.0 Hz, $^4J(H_3H_5)$ = 1.5 Hz, 1H, H_5), 6.77 (d, $^4J(PH)$ = 7.0 Hz, 1H, H_1), 6.09 (ddddd, $^3J(H_aH_c)$ = 17.5 Hz, $^3J(H_aH_b)$ = 10.0 Hz, $^3J(H_aCH_2)$ = 7.8 Hz, $^3J(H_aCH_2)$ = 7.0 Hz, $^3J(PH)$ = 6.0 Hz, 1H, H_a), 5.08 (ddd, $^3J(H_aH_b)$ = 10.0 Hz, $^4J(PH)$ = 3.5 Hz, $^2J(H_bH_c)$ = 1.5 Hz, 1H, H_b), 4.91 (ddd, $^3J(H_aH_c)$ = 17.5 Hz, $^4J(PH)$ = 5.0 Hz, $^2J(H_bH_c)$ = 1.5 Hz, 1H, H_c), 3.94 (qd, $^3J(HH)$ = 6.5 Hz, $^4J(PH)$ = 1.5 Hz, 1H, CH), 3.60 (apparent td, $^2J(PH)$ = $^2J(HH)$ = 13.0 Hz, $^3J(CH_2H_a)$ = 7.0 Hz, 1H, $CH_{2(a)}$), 3.40 (apparent td, $^2J(PH)$ = $^2J(HH)$ = 13.0 Hz, $^3J(CH_2H_a)$ = 7.8 Hz, 1H, $CH_{2(b)}$), 2.80 (d, $^4J(PH)$ = 2.0 Hz, 3H, NCH_3), 2.78 (d, $^4J(PH)$ = 3.0 Hz, 3H, NCH_3), 1.87 (d, $^3J(HH)$ = 6.5 Hz, 3H, CCH_3). Assignments were made with the aid of $^1H\{^1H$ sel.$\}$, $^1H\{^{31}P\}$, and COSY-45 experiments. $^{13}C\{^1H\}$ NMR (125.7 MHz, $CDCl_3$, 25 °C): δ 152.68 (d, $^2J(PC)$ = 2.1 Hz, C_1), 148.76 (s, C_{10}), 135.98 (d, $^3J(PC)$ = 11.4 Hz, C_2), 134.23 (d, $^2J(PC)$ = 11.3 Hz, C_o), 134.03 (d, $^2J(PC)$ = 10.6 Hz, C_o), 131.93 (d, $^4J(PC)$ = 6.0 Hz, C_3), 131.46 (d, $^2J(PC)$ = 5.0 Hz, C_α), 130.85 (s, C_8), 130.72 (d, $^4J(PC)$ = 2.6 Hz, C_p), 130.49 (d, $^1J(PC)$ = 45.5 Hz, C_i), 130.46 (d, $^4J(PC)$ = 2.5 Hz, C_p), 130.32 (d, $^1J(PC)$ = 45.3 Hz, C_i), 128.36 (d, $^3J(PC)$ = 10.4 Hz, C_m), 128.06 (d, $^3J(PC)$ = 10.4 Hz, C_m), 126.77 (s, C_4), 126.74 (s, C_7), 124.66 (s, C_6), 124.40 (s, C_5), 119.88 (s, C_9), 119.33 (d, $^3J(PC)$ = 12.1 Hz, C_β), 74.60 (d, $^4J(PC)$ = 3.1 Hz, CH), 50.09 (d, $^3J(PC)$ = 3.0 Hz, NCH_3), 46.13 (d, $^3J(PC)$ = 2.4 Hz, NCH_3), 36.14 (d, $^1J(PC)$ = 31.3 Hz, CH_2), 20.94 (s, CCH_3). Assignments were made with the aid of APT and $^{13}C/^1H$ HETCOR experiments.

(*S*$_C$)-5: mp 185−187 °C; $[\alpha]_D$ +29.2° (*c* 0.5, CH_2Cl_2); 3.35 g (94% yield). Anal. Calcd for $C_{25}H_{29}ClNPPd$: C, 58.15; H, 5.62; Cl, 6.87. Found: C, 58.03; H, 5.55; Cl, 6.72. IR (CsI): ν_{Pd-Cl} 299 cm^{-1} (shp, st). $^{31}P\{^1H\}$ NMR (202.3 MHz, $CDCl_3$, 25 °C):

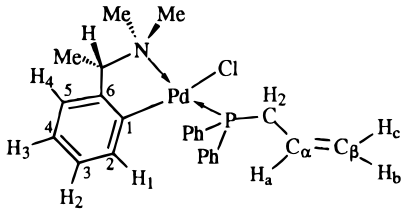

δ 37.59 (s, 1P, ADPP). ^{1}H NMR (499.8 MHz, $CDCl_3$, 25 °C): δ 7.90 (m, 2H, H_o), 7.68 (m, 2H, H_o), 7.42 (m, 4H, H_m), 7.30 (m, 2H, H_p), 6.92 (dd, $^3J(H_3H_4) = 7.5$ Hz, $^4J(H_2H_4) = 1.0$ Hz, 1H, H_4), 6.81 (ddd, $^3J(H_2H_3) = 8.0$ Hz, $^3J(H_3H_4) = 7.5$ Hz, $^4J(H_1H_3) = 3.2$ Hz, 1H, H_3), 6.44 (m, 2H, H_1, H_2), 6.00 (ddddd, $^3J(H_aH_c) = 17.0$ Hz, $^3J(H_aH_b) = 10.5$ Hz, $^3J(H_aCH_2) = 8.0$ Hz, $^3J(H_a$-$CH_2) = 7.0$ Hz, $^3J(PH) = 6.0$ Hz, 1H, H_a), 5.02 (ddd, $^3J(H_aH_b) = 10.5$ Hz, $^4J(PH) = 3.0$ Hz, $^2J(H_bH_c) = 1.5$ Hz, 1H, H_b), 4.81 (ddd, $^3J(H_aH_c) = 17.0$ Hz, $^4J(PH) = 5.0$ Hz, $^2J(H_bH_c) = 1.5$ Hz, 1H, H_c), 3.77 (qd, $^3J(HH) = 6.5$ Hz, $^4J(PH) = 4.5$ Hz, 1H, CH), 3.54 (apparent td, $^2J(PH) = {}^2J(HH) = 13.0$ Hz, $^3J(CH_2H_a) = 7.0$ Hz, 1H, $CH_{2(a)}$), 3.29 (apparent td, $^2J(PH) = {}^2J(HH) = 13.0$ Hz, $^3J(CH_2H_a) = 8.0$ Hz, 1H, $CH_{2(b)}$), 2.77 (d, $^4J(PH) = 2.0$ Hz, 3H, NCH_3), 2.75 (d, $^4J(PH) = 3.0$ Hz, 3H, NCH_3), 1.76 (d, $^3J(HH) = 6.5$ Hz, 3H, CCH_3). $^{13}C\{^1H\}$ NMR (125.7 MHz, $CDCl_3$, 25 °C): δ 154.16 (d, $^2J(PC) = 2.0$ Hz, C_1), 150.60 (s, C_6), 137.15 (d, $^3J(PC) = 11.3$ Hz, C_2), 134.11 (d, $^2J(PC) = 11.3$ Hz, C_o), 134.02 (d, $^2J(PC) = 10.9$ Hz, C_o), 131.26 (d, $^2J(PC) = 5.0$ Hz, C_α), 130.62 (d, $^4J(PC) = 2.3$ Hz, C_p), 130.39 (d, $^4J(PC) = 2.6$ Hz, C_p), 130.28 (d, $^1J(PC) = 45.1$ Hz, C_i), 130.25 (d, $^1J(PC) = 44.9$ Hz, C_i), 128.28 (d, $^3J(PC) = 10.3$ Hz, C_m), 127.94 (d, $^3J(PC) = 10.3$ Hz, C_m), 125.09 (d, $^4J(PC) = 6.0$ Hz, C_3), 123.74 (s, C_4), 122.17 (s, C_5), 119.19 (d, $^3J(PC) = 12.1$ Hz, C_β), 74.99 (d, $^3J(PC) = 3.4$ Hz, CH), 50.04 (d, $^3J(PC) = 3.0$ Hz, NCH_3), 46.12 (d, $^3J(PC) = 2.3$ Hz, NCH_3), 36.38 (d, $^1J(PC) = 30.9$ Hz, CH_2), 21.29 (s, CCH_3).

(S_C)-6: mp 186−188 °C; $[\alpha]_D$ +26.8° (*c* 0.2, CH_2Cl_2); 2.93 g (94.5% yield). Anal. Calcd for $C_{26}H_{29}ClNPPd$: C, 62.81; H, 5.83; Cl, 7.13. Found: C, 62.73; H, 5.69; Cl, 7.02. IR (CsI): ν_{Pd-Cl} 294 cm^{-1} (shp, st). $^{31}P\{^1H\}$ NMR (202.3 MHz, $CDCl_3$, 25 °C):

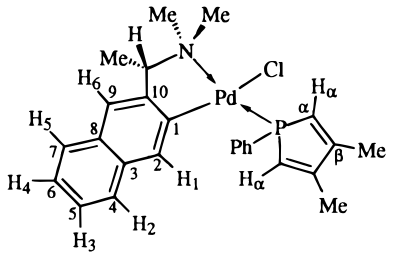

δ 37.28 (s, 1P, DMPP). ^{1}H NMR (499.8 MHz, $CDCl_3$, 25 °C): δ 7.97 (m, 2H, H_o), 7.68 (dd, $^3J(H_2H_3) = 8.0$ Hz, $^4J(H_2H_4) = 1.5$ Hz, 1H, H_2), 7.45 (s, H_6), 7.42 (m, 3H, $H_{m,\ p}$), 7.41 (dd, $^3J(H_4H_5) = 8.0$ Hz, $^4J(H_3H_5) = 1.5$ Hz, 1H, H_5), 7.33 (ddd, $^3J(H_2H_3) = 8.0$ Hz, $^3J(H_3H_4) = 7.0$ Hz, $^4J(H_3H_5) = 1.5$ Hz, 1H, H_3), 7.33 (d, $^4J(PH) = 6.5$ Hz, 1H, H_1), 7.30 (ddd, $^3J(H_4H_5) = 8.0$ Hz, $^3J(H_3H_4) = 7.0$ Hz, $^4J(H_2H_4) = 1.5$ Hz, 1H, H_4), 6.78 (d, $^2J(PH) = 32.0$ Hz, 1H, H_α), 6.68 (d, $^2J(PH) = 32.5$ Hz, 1H, H_α), 4.01 (qd, $^3J(HH) = 6.5$ Hz, $^4J(PH) = 2.0$ Hz, 1H, CH), 2.87 (d, $^4J(PH) = 2.0$ Hz, 3H, NCH_3), 2.72 (d, $^4J(PH) = 3.0$ Hz, 3H, NCH_3), 2.09 (s, 3H, DMPP-Me), 2.08 (s, 3H, DMPP-Me), 1.71 (d, $^3J(HH) = 6.5$ Hz, 3H, CMe). Our previously reported assignments[3j] are partially incorrect. $^{13}C\{^1H\}$ NMR (125.7 MHz, $CDCl_3$, 25 °C): δ 152.77 (d, $^2J(PC) = 1.8$ Hz, C_1), 152.42 (d, $^2J(PC) = 11.1$ Hz, C_β), 151.57 (d, $^2J(PC) = 11.7$ Hz, C_β), 146.88 (d, $^3J(PC) = 2.8$ Hz, C_{10}), 135.43 (d, $^3J(PC) = 12.9$ Hz, C_2), 133.85 (d, $^2J(PC) = 12.8$ Hz, C_o), 132.11 (d, $^4J(PC) = 6.2$ Hz, C_3), 131.15 (s, C_8), 130.96 (d, $^4J(PC) = 2.5$ Hz, C_p), 128.73 (d, $^3J(PC) = 11.1$ Hz, C_m), 127.13 (s, C_4), 126.71 (d, $^1J(PC) = 46.9$ Hz, C_i), 126.67 (s, C_7), 126.61 (d, $^1J(PC) = 52.7$ Hz, C_α), 125.74 (d, $^1J(PC) = 52.2$ Hz, C_α), 125.17 (s, C_6), 124.69 (s, C_5), 120.96 (s, C_9), 74.12 (d, $^3J(PC) = 3.1$ Hz, CH), 49.82 (d, $^3J(PC) = 2.9$ Hz, NMe), 45.23 (d, $^3J(PC) = 2.3$ Hz, NMe), 19.52 (s, CMe), 17.75 (d, $^3J(PC) = 2.6$ Hz, DMPP-Me), 17.65 (d, $^3J(PC) = 2.6$ Hz, DMPP-Me).

(S_C)-4: mp 140−142 °C; $[\alpha]_D$ +96° (*c* 0.5, CH_2Cl_2); 3.13 g (95% yield). Anal. Calcd for $C_{22}H_{27}ClNPPd$: C, 55.27; H, 5.65; Cl, 7.42. Found: C, 55.19; H, 5.47; Cl, 7.34. IR (CsI): ν_{Pd-Cl} 296 cm^{-1} (shp, st). $^{31}P\{^1H\}$ NMR (202.3 MHz, $CDCl_3$, 25 °C):

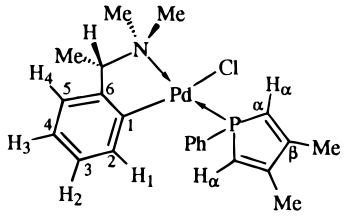

δ 42.10 (s, 1P, DMPP). ^{1}H NMR (499.8 MHz, $CDCl_3$, 25 °C): δ 7.88 (m, 2H, H_o), 7.41 (m, 1H, H_p), 7.35 (m, 2H, H_m), 6.99 (m, 2H, H_3, H_4), 6.92 (apparent td $^3J(H_1H_2) = {}^4J(PH) = 7.0$ Hz, $^4J(H_1H_3) = 0.5$ Hz, 1H, H_1), 6.81 (apparent td $^3J(H_1H_2) = {}^3J(H_2H_3) = 7.0$ Hz, $^4J(H_2H_4) = 2.0$ Hz, 1H, H_2), 6.75 (d, $^2J(PH) = 32.5$ Hz, 1H, H_α), 6.61 (d, $^2J(PH) = 32.5$ Hz, 1H, H_α), 3.84 (qd, $^3J(HH) = 7.0$ Hz, $^4J(PH) = 4.0$ Hz, 1H, CH), 2.85 (d, $^4J(PH) = 2.0$ Hz, 3H, NCH_3), 2.70 (d, $^4J(PH) = 3.0$ Hz, 3H, NCH_3), 2.08 (s, 3H, DMPP-Me), 2.07 (s, 3H, DMPP-Me), 1.60 (d, $^3J(HH) = 7.0$ Hz, 3H, CMe). $^{13}C\{^1H\}$ NMR (125.7 MHz, $CDCl_3$, 25 °C): δ 154.65 (d, $^2J(PC) = 2.0$ Hz, C_1), 152.44 (d, $^2J(PC) = 10.9$ Hz, C_β), 151.32 (d, $^2J(PC) = 10.6$ Hz, C_β), 148.49 (d, $^3J(PC) = 2.8$ Hz, C_6), 136.93 (d, $^3J(PC) = 12.6$ Hz, C_2), 133.84 (d, $^2J(PC) = 13.1$ Hz, C_o), 130.86 (d, $^4J(PC) = 2.6$ Hz, C_p), 128.62 (d, $^3J(PC) = 10.9$ Hz, C_m), 126.80 (d, $^1J(PC) = 52.4$ Hz, C_α), 126.47 (d, $^1J(PC) = 46.4$ Hz, C_i), 125.72 (d, $^1J(PC) = 51.8$ Hz, C_α), 125.58 (d, $^4J(PC) = 5.9$ Hz, C_3), 124.21 (s, C_4), 123.16 (s, C_5), 74.52 (d, $^3J(PC) = 3.0$ Hz, CH), 49.87 (d, $^3J(PC) = 2.9$ Hz, NMe), 45.32 (d, $^3J(PC) = 2.5$ Hz, NMe), 20.11 (s, CMe), 17.70 (s, DMPP-Me), 17.60 (s, DMPP-Me). Assignments were made with the aid of $^1H\{^1H$ sel.$\}$, $^1H\{^{31}P\}$, COSY-45, APT, and ^{13}C/^1H HETCOR experiments.

(S_C)-8. To a stirred solution of (S_C)-**4** 0.83 g (1.74 mmol) in distilled CH_3CN (40 mL) under nitrogen was added 0.29 g (1.74 mmol) of $AgNO_3$, and the reaction mixture was stirred for 6 h. Since $AgNO_3$ is light sensitive, the reaction was performed in the dark. The resulting mixture was filtered through a layer of Celite to remove AgCl. The pale yellow colored filtrate was then taken to dryness on a rotary evaporator to give an opaque colored solid residue. The solid residue was dissolved in a minimum amount of CH_3CN, and an acetone/diethyl ether mixture (1:5) was slowly added to give (S_C)-**8** as colorless prisms: mp 199−201 °C (blackens at 175 °C); $[\alpha]_D$ +67.6° (*c* 0.5, CH_2Cl_2); 0.82 g (95% yield). Anal. Calcd for $C_{22}H_{27}N_2O_3PPd$: C, 52.36; H, 5.35. Found: C, 52.21; H, 5.40. IR (KBr): $\nu_{(NO)}$ 1450 cm^{-1} (b, st), 1282 cm^{-1} (b, st) and 1019 cm^{-1} (b, st). $^{31}P\{^1H\}$ NMR (202.3 MHz, $CDCl_3$, 25 °C): δ 40.90 (s, 1P, DMPP). ^{1}H NMR (499.8 MHz, $CDCl_3$, 25 °C): δ 7.84 (m, 2H, H_o), 7.44 (m, 1H, H_p), 7.35 (m, 2H, H_m), 6.97 (m, 2H, H_3, H_4), 6.75 (m, 2H, H_1, H_2), 6.44 (ddq, $^2J(PH) = 34.0$ Hz, $^4J(H_\alpha H_{\alpha'}) = 2.5$ Hz, $^4J(HH) = 1.0$ Hz, 1H, H_α), 6.39 (ddq, $^2J(PH) = 34.0$ Hz, $^4J(H_\alpha H_{\alpha'}) = 2.5$ Hz, $^4J(HH) = 1.0$ Hz, 1H, H_α), 3.86 (qd, $^3J(HH) = 7.0$ Hz, $^4J(PH) = 4.0$ Hz, 1H, CH), 2.82 (d, $^4J(PH) = 2.5$ Hz, 3H, NCH_3), 2.60 (d, $^4J(PH) = 3.0$ Hz, 3H, NCH_3), 2.10 (d, $^4J(HH) = 1.0$ Hz, 6H, DMPP−Me), 1.62 (d, $^3J(HH) = 7.0$ Hz, 3H, CMe). $^{13}C\{^1H\}$ NMR (125.7 MHz, $CDCl_3$, 25 °C): δ 154.52 (d, $^2J(PC) = 1.9$ Hz, C_1), 153.41 (d, $^2J(PC) = 10.4$ Hz, C_β), 153.11 (d, $^2J(PC) = 10.1$ Hz, C_β), 141.68 (d, $^3J(PC) = 5.5$ Hz, C_6), 137.04 (d, $^3J(PC) = 13.1$ Hz, C_2), 133.73 (d, $^2J(PC) = 13.4$ Hz, C_o), 131.21 (d, $^4J(PC) = 2.5$ Hz, C_p), 128.72 (d, $^3J(PC) = 11.3$ Hz, C_m), 125.81 (d, $^4J(PC) = 5.5$ Hz, C_3), 125.14 (d, $^1J(PC) = 48.0$ Hz, C_i), 124.66 (s, C_4), 124.31 (d, $^1J(PC) = 49.1$ Hz, C_α), 124.15 (d, $^1J(PC) = 49.8$ Hz, C_α), 123.29 (s, C_5), 73.30

(d, ^3J(PC) = 3.0 Hz, CH), 49.62 (d, ^3J(PC) = 2.5 Hz, NMe), 44.20 (d, ^3J(PC) = 2.1 Hz, NMe), 19.95 (s, CMe), 17.71 (d, ^3J(PC) = 4.9 Hz, DMPP−Me), 17.61 (d, ^3J(PC) = 4.9 Hz, DMPP−Me).

Synthesis and Characterization of [(DMPP)$_4$Pd](X)$_2$; X = PF$_6^-$, 9; X = ClO$_4^-$, 9a; and {[(DMPP)(CH$_3$CN)L-*C*,*N*]-palladium(II)}(X) ([(*S*$_C$)-10], L = TMBA, X = PF$_6^-$; [(*S*$_C$)-10a], L = TMBA, X = ClO$_4^-$; [(*S*$_C$)-11], L = TMNA, X = PF$_6^-$; [(*S*$_C$)-11a], L = TMNA, X = ClO$_4^-$). Method a. Both the reactions of enantiomerically pure complexes (*S*$_C$)-**1a** and (*S*$_C$)-**2a** with 1-phenyl-3,4-dimethylphosphole (DMPP) in the presence of $NaPF_6$ as a chloride scavenger gave the same result as illustrated in Scheme 2. In each reaction, [(DMPP)$_4$Pd](PF$_6$)$_2$ was separated from the bulk product by fractional crystallization. Dissolution of the remaining product in CH_3CN and slow addition of an acetone/diethyl ether mixture resulted in the formation of the complexes (*S*$_C$)-**10** and (*S*$_C$)-**11**, respectively. The following preparation and isolation of [(DMPP)$_4$Pd](PF$_6$)$_2$, **9**, and complex (*S*$_C$)-**11** is representative.

[(DMPP)$_4$Pd](PF$_6$)$_2$, 9, and (S$_C$)-11. To 0.5 g (0.735 mmol) of (*S*$_C$)-**2a** in CH_2Cl_2 (50 mL) under nitrogen were added 0.70 mL (3.68 mmol) of DMPP via syringe and 0.65 g (3.87 mmol) of $NaPF_6$. The reaction mixture was stirred magnetically for 3 days at ambient temperature. As the reaction proceeded, the original yellow color of the solution gradually changed to orange. The resulting orange-colored solution was filtered through a layer of Celite to remove NaCl, excess $NaPF_6$, and any elemental palladium that formed. The filtrate was then taken to dryness on a rotary evaporator. The resulting foamy red solid was washed with several small portions of a hexane/diethyl ether (1:1) mixture and crystallized from acetone/diethyl ether to afford pale yellow prisms. The crystals obtained (0.51 g) were shown by $^{31}P\{^1H\}$ and ^1H NMR spectroscopy to be [(DMPP)$_4$Pd](PF$_6$)$_2$: mp 234−236 °C (blackens at 200 °C). Anal. Calcd for $C_{48}H_{52}F_{12}P_6Pd$: C, 49.40; H, 4.53; Found: C, 49.28; H, 4.46. $^{31}P\{^1H\}$ NMR (202.3 MHz, CD_3NO_2, 25 °C): δ 21.96 (s, 4P, DMPP), −145.0 (sept, ^1J(PF) = 707 Hz, 2P, PF_6^-). ^1H NMR (499.8 MHz, CD_3NO_2, 25 °C): δ 7.62 (m, 4H, H$_p$), 7.47 (m, 16H, H$_{o,\,m}$), 6.47 ([AX$_2$]$_4$, $|^2J(PH) + {}^4J(PH)|$ = 39.0 Hz, 8H, H$_\alpha$), 1.86 (s, 24H, CH$_3$). $^{13}C\{^1H\}$ NMR (125.7 MHz, CD_3NO_2, 25 °C): δ 159.60 (A[X]$_4$, $|^2J(PC) + {}^4J(PC)|$ = 13.1 Hz, C$_\beta$), 133.03 (s, C$_p$), 131.56 (A[X]$_4$, $|^2J(PC) + {}^4J(PC)|$ = 14.7 Hz, C$_o$), 129.82 (A[X]$_4$, $|^3J(PC) + {}^5J(PC)|$ = 12.4 Hz, C$_m$), 123.43 (A[X]$_4$, $|^1J(PC) + {}^3J(PC)|$ = 59.1 Hz, C$_i$), 121.10 (A[X]$_4$, $|^1J(PC) + {}^3J(PC)|$ = 74.9 Hz, C$_\alpha$), 16.75 (A[X]$_4$, $|^3J(PC) + {}^5J(PC)|$ = 13.7 Hz, DMPP−CH$_3$).

After separating [(DMPP)$_4$Pd](PF$_6$)$_2$ from the acetone/diethyl ether solution of the bulk product by filtration the solvents were removed via rotary evaporation and the resulting red solid residue was dissolved in a minimum amount of CH_3CN. Slow addition of acetone/diethyl ether (1:2) to the CH_3CN solution resulted in the formation of pale yellow crystals after 2 days standing at ambient temperature. The resulting crystals were isolated by filtration and washed with several small portions of a hexane/diethyl ether mixture. Drying the resulting solid in vacuo gave the complex (*S*$_C$)-**11** as a pale yellow crystalline solid: mp 188−190 °C (blackens at 180 °C); $[\alpha]_D$ +50.4° (*c* 0.5, CH_2Cl_2); 0.65 g (65% yield). Anal. Calcd for $C_{28}H_{32}F_6N_2P_2Pd$: C, 42.84; H, 4.08. Found: C, 42.71; H, 3.99. IR (KBr): $\nu_{(CN)}$ 2312 cm^{-1} (shp, st) and 2285 cm^{-1} (shp, st). $^{31}P\{^1H\}$ NMR (202.3 MHz, acetone-d_6, 25 °C): δ 32.83 (s, 1P, DMPP), −145.0 (sept, ^1J(PF) = 708 Hz, 1P, PF_6^-). ^1H NMR (499.8 MHz, acetone-d_6, 25 °C): δ 7.90 (m, 2H, H$_o$), 7.76 (dd, $^3J(H_2H_3)$ = 8.0 Hz, $^4J(H_2H_4)$ = 1.0 Hz, 1H, H$_2$), 7.61 (s, 1H, H$_6$), 7.56 (m, 1H, H$_p$), 7.50 (m, 2H, H$_m$), 7.40 (dd, $^3J(H_4H_5)$ = 8.0 Hz, $^4J(H_3H_5)$ = 1.0 Hz, 1H, H$_5$), 7.38 (ddd, $^3J(H_2H_3)$ = 8.0 Hz, $^3J(H_3H_4)$ = 7.0 Hz, $^4J(H_3H_5)$ = 1.0 Hz, 1H, H$_3$), 7.32 (ddd, $^3J(H_4H_5)$ = 8.0 Hz, $^3J(H_3H_4)$ = 7.0 Hz, $^4J(H_2H_4)$ = 1.0 Hz, 1H, H$_4$), 7.26 (d, ^4J(PH) = 7.0 Hz, 1H, H$_1$), 6.78 (d, ^2J(PH) = 35.0 Hz, 1H, H$_\alpha$), 6.71 (d, ^2J(PH) = 32.5 Hz, 1H, H$_\alpha$), 4.22 (qd, ^3J(HH) = 6.5 Hz, ^4J(PH) = 6.0 Hz, 1H, CH), 2.88 (d, ^4J(PH) = 2.5 Hz, 3H, NMe), 2.75 (d, ^4J(PH) = 3.0 Hz, 3H, NMe), 2.36 (s, 3H, CH_3CN), 2.25 (s, 3H, DMPP-Me), 2.24 (s, 3H, DMPP-Me), 1.79 (d, ^3J(HH) = 6.5 Hz, 3H, CMe). PH couplings were confirmed by a $^1H\{^{31}P\}$ experiment. $^{13}C\{^1H\}$ NMR (202.3 MHz, acetone-d_6, 25 °C): δ 156.32 (d, ^2J(PC) = 10.4 Hz, C$_\beta$), 156.10 (d, ^2J(PC) = 10.1 Hz, C$_\beta$), 153.82 (d, ^2J(PC) = 2.1 Hz, C$_1$), 141.85 (d, ^3J(PC) = 6.3 Hz, C$_{10}$), 136.56 (d, ^3J(PC) = 13.8 Hz, C$_2$), 134.62 (d, ^2J(PC) = 12.9 Hz, C$_o$), 133.20 (d, ^1J(PC) = 5.9 Hz, C$_i$), 132.81 (s, C$_8$), 132.76 (d, ^4J(PC) = 2.5 Hz, C$_3$), 130.18 (d, ^3J(PC) = 11.3 Hz, C$_m$), 128.19 (s, C$_4$), 127.78 (s, C$_7$), 126.48 (s, C$_6$), 126.35 (s, C$_5$), 126.08 (s, CH_3CN), 124.79 (d, ^1J(PC) = 49.9 Hz, C$_\alpha$), 124.66 (d, ^1J(PC) = 50.7 Hz, C$_\alpha$), 122.69 (s, C$_9$), 74.34 (d, ^3J(PC) = 3.0 Hz, CH), 50.73 (s, NMe), 46.15 (s, NMe), 20.97 (s, CMe), 17.84 (d, ^3J(PC) = 4.7 Hz, DMPP-Me), 17.74 (d, ^3J(PC) = 5.0 Hz, DMPP-Me), 2.25 (s, CH_3CN). Assignments were aided by APT and $^{13}C/^1H$ HETCOR experiments.

(*S*$_C$)-10: mp 178−180 °C (blackens at 170 °C); $[\alpha]_D$ +64.8° (*c* 0.5, CH_2Cl_2); 0.68 g (62.7% yield). Anal. Calcd for $C_{24}H_{30}F_6N_2P_2Pd$: C, 39.22; H, 4.08. Found: C, 39.09; H, 3.95. IR (KBr): $\nu_{(CN)}$ 2312 cm^{-1} (shp, st) and 2285 cm^{-1} (shp, st). $^{31}P\{^1H\}$ NMR (202.3 MHz, $CDCl_3$, 25 °C): δ 33.22 (s, 1P, DMPP), −145.0 (sept, ^1J(PF) = 711 Hz, 1P, PF_6^-). ^1H NMR (499.8 MHz, $CDCl_3$, 25 °C): δ 7.70 (m, 2H, H$_o$), 7.48 (m, 1H, H$_p$), 7.42 (m, 2H, H$_m$), 7.02 (m, 2H, H$_3$, H$_4$), 6.79 (ddd, $^3J(H_1H_2)$ = 7.5 Hz, $^3J(H_2H_3)$ = 6.0 Hz, $^4J(H_2H_4)$ = 3.5 Hz, 1H, H$_2$), 6.72 (dd, $^3J(H_1H_2)$ = 7.5 Hz, ^4J(PH) = 6.5 Hz, 1H, H$_1$), 6.43 (d, ^2J(PH) = 35.0 Hz, 1H, H$_\alpha$), 6.41 (d, ^2J(PH) = 35.0 Hz, 1H, H$_\alpha$), 3.83 (qd, ^3J(HH) = 6.5 Hz, ^4J(PH) = 4.5 Hz, 1H, CH), 2.85 (d, ^4J(PH) = 2.0 Hz, 3H, NMe), 2.72 (d, ^4J(PH) = 3.0 Hz, 3H, NMe), 2.34 (s, 3H, CH_3CN), 2.19 (s, 3H, DMPP−Me), 2.17 (s, 3H, DMPP−Me), 1.64 (d, ^3J(HH) = 6.5 Hz, 3H, CMe). PH couplings were confirmed by a $^1H\{^{31}P\}$ experiment. $^{13}C\{^1H\}$ NMR (202.3 MHz, $CDCl_3$, 25 °C): δ 154.94 (d, ^2J(PC) = 2.1 Hz, C$_1$), 154.44 (d, ^2J(PC) = 11.6 Hz, C$_\beta$), 154.08 (d, ^2J(PC) = 9.0 Hz, C$_\beta$), 142.70 (s, C$_6$), 134.64 (d, ^3J(PC) = 13.6 Hz, C$_2$), 133.71 (d, ^2J(PC) = 13.4 Hz, C$_o$), 131.75 (d, ^4J(PC) = 2.4 Hz, C$_p$), 129.10 (d, ^3J(PC) = 11.4 Hz, C$_m$), 126.11 (d, ^4J(PC) = 6.0 Hz, C$_3$), 125.49 (s, CH_3CN), 124.61 (d, ^1J(PC) = 50.2 Hz, C$_\alpha$), 124.20 (d, ^1J(PC) = 51.8 Hz, C$_\alpha$, C$_i$), 123.66 (s, C$_5$), 73.96 (d, ^3J(PC) = 2.8 Hz, CH), 50.35 (d, ^3J(PC) = 1.8 Hz, NMe), 45.84 (s, NMe), 20.74 (s, CMe), 17.75 (d, ^3J(PC) = 3.0 Hz, DMPP−Me), 17.65 (d, ^3J(PC) = 5.0 Hz, DMPP−Me), 2.78 (s, CH_3CN). Assignments were aided by APT and $^{13}C/^1H$ HETCOR experiments.

It is noteworthy that performing the reactions in CH_3CN resulted in the formation of complexes (*S*$_C$)-**10** and (*S*$_C$)-**11** only as shown in Scheme 2.

Method b. As illustrated in Scheme 3, both the reactions of the chloro complexes (*S*$_C$)-**4** and (*S*$_C$)-**6** with $AgClO_4$ and removal of the AgCl by filtration, followed by addition of DMPP via syringe, produced [(DMPP)$_4$Pd](ClO$_4$)$_2$. In each reaction, [(DMPP)$_4$Pd](ClO$_4$)$_2$ was separated from the bulk products by fractional crystallization. Dissolution of the remaining products in CH_3CN followed by slow addition of an acetone/diethyl ether mixture resulted in the formation of the complexes (*S*$_C$)-**10a** and (*S*$_C$)-**11a**. The following preparations of [(DMPP)$_4$Pd](ClO$_4$)$_2$ and (*S*$_C$)-**11a** are representative.

[(DMPP)$_4$Pd](ClO$_4$)$_2$, 9a, and (S$_C$)-11a. To 0.5 g (0.947 mmol) of (S$_C$)-**6** in CH_2Cl_2 (50 mL) under nitrogen were added 0.50 g (2.41 mmol) of $AgClO_4$, and the reaction mixture was stirred magnetically for 45 min. The resulting mixture was filtered through a layer of Celite to remove AgCl. To the pale yellow filtrate under nitrogen was added 0.25 mL (1.33 mmol) of DMPP via syringe, and the reaction mixture was stirred magnetically for 3 days at ambient temperature. The solvent was removed under reduced pressure to give a red foamy residue. The residue was washed with several small portions of a hexane/diethyl ether (1:1) mixture. The remaining red solid was dissolved in a minimum amount of acetone, and diethyl ether was added to crystallize [(DMPP)$_4$Pd](ClO$_4$)$_2$ as pale yellow prisms that were isolated by filtration and dried in vacuo. The crystals obtained (0.30 g) were shown by ^{31}P-

{^{1}H} and ^{1}H NMR spectroscopy to be $[(DMPP)_4Pd](ClO_4)_2$, **9a**: mp 238−240 °C (blackens at 210 °C). Anal. Calcd for $C_{48}H_{52}Cl_2O_8P_4Pd$: C, 49.52; H, 4.47. Found: C, 49.54; H, 4.38. The ^{1}H, ^{13}C{^{1}H}, and ^{31}P{^{1}H} NMR spectral data are essentially the same (except for the absence of a PF_6^- resonance in the latter) as those of **9**. A crystal structure was also obtained: orthorhombic, *Pbca*, $a = 18.2430(14)$ Å, $b = 14.817(2)$ Å, $c = 18.4497(11)$ Å, $\alpha = \beta = \gamma = 90°$, $V = 4987.0(7)$ Å^3, $Z = 4$, $\rho_{calc} = 1.409$ g cm^{-3}. Refinement converged to R1(F) = 0.0583, wR2(F^2) = 0.1213 for 4383 independent observed reflections [$I > 2\sigma(I)$]. The metrical parameters for the cation are essentially the same as those reported for **9**.

The red-purple colored filtrate was then taken to dryness on a rotary evaporator to give an orange-red solid residue. The solid residue was dissolved in a minimum amount of CH_3CN, and an acetone/diethyl ether mixture (1:2) was slowly added to give (S_C)-**11a** as a pale yellow crystalline solid. The product was isolated by filtration, washed with several small portions of a hexane/diethyl ether (1:1) mixture, and air-dried. The solid was recrystallized from CH_3CN/Et_2O, forming pale yellow prisms: mp 192−194 °C (blackens at 185 °C); $[\alpha]_D$ +48° (*c* 0.5, CH_2Cl_2); 0.39 g (64.3% yield). Anal. Calcd for $C_{28}H_{32}ClN_2O_4PPd$: C, 45.47; H, 4.33. Found: C, 45.38; H, 4.24. IR (KBr): $\nu_{(CN)}$ 2309 cm^{-1} (shp, st) and 2281 cm^{-1} (shp, st). The ^{1}H, ^{13}C{^{1}H}, and ^{31}P{^{1}H} NMR spectral data are essentially the same (except for the absence of a PF_6^- resonance in the latter) as those of (S_C)-**11**.

(S_C)-10a: mp 182−184 °C (blackens at 175 °C); $[\alpha]_D$ +71.2° (*c* 0.5, CH_2Cl_2); 0.38 g (62% yield). Anal. Calcd for $C_{24}H_{30}ClN_2O_4PPd$: C, 41.81; H, 4.35. Found: C, 41.65; H, 4.26. IR (KBr): $\nu_{(CN)}$ 2311 cm^{-1} (shp, st) and 2283 cm^{-1} (shp, st). The ^{1}H, ^{13}C{^{1}H}, and ^{31}P{^{1}H} NMR spectral data are essentially the same (except for the absence of a PF_6^- resonance in the latter) as those of (S_C)-**10**.

[(DMPP-[2+2])$_2$Pd](PF$_6$)$_2$, 12. A 0.5 g sample of **9** was sealed in an ampule and heated in an oven at 145 °C for 1 week. The colorless solid became pale red during this period. Dissolution of the solid in acetone followed by slow addition of diethyl ether afforded 0.24 g (48% yield) of colorless crystals: mp 200−202 °C (blackens at 185 °C). Anal. Calcd for $C_{48}H_{52}F_{12}P_6Pd$: C, 49.40; H, 4.53. Found: C, 49.17; H, 4.39.

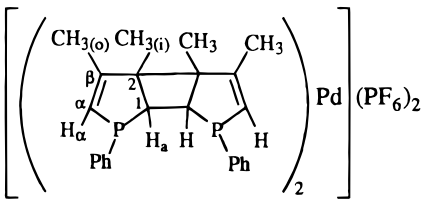

^{31}P{^{1}H} NMR (202.3 MHz, CD_3NO_2, 25 °C): δ 89.80 (s, 4P, ligand), −145.0 (sept, ^1J(PF) = 707 Hz, 2P, PF_6^-). ^{1}H NMR (499.8 MHz, CD_3NO_2, 25 °C): δ 7.53 (m, 4H, H_p), 7.39 (m, 8H, H_m), 7.22 (m, 8H, H_o), 5.95 ([AX]$_2$, $|^2J(PH) + {}^4J(PH)| = 29.0$ Hz, 4H, H_α), 3.44 ([AX]$_2$, $|^2J(PH) + {}^3J(PH)| = 20.5$ Hz, 4H, H_a), 2.08 (m, 12H, $CH_{3(o)}$), 1.49 (s, 12H, $CH_{3(i)}$). ^{13}C{^{1}H} NMR (125.7 MHz, CD_3NO_2, 25 °C): δ 167.86 (A[X]$_4$, $|^2J(PC) + {}^4J(PC)| = 5.3$ Hz, C_β), 132.23 (s, C_p), 131.56 (A[X]$_4$, $|^1J(PC) + {}^3J(PC)| = 51.8$ Hz, C_i), 130.51 (A[X]$_4$, $|^2J(PC) + {}^4J(PC)| = 6.9$ Hz, C_o), 129.33 (A[X]$_4$, $|^3J(PC) + {}^5J(PC)| = 4.8$ Hz, C_m), 115.80 (A[X]$_4$, $|^1J(PC) + {}^3J(PC)| = 47.8$ Hz, C_α), 70.65 (A[X]$_4$, $|^2J(PC) + {}^3J(PC)| = 4.3$ Hz, C_2), 53.27 (A[X]$_4$, $|^1J(PC) + {}^2J(PC)| = 23.4$ Hz, C_1), 20.4 (s, $CH_{3(i)}$), 17.66 (A[X]$_4$, $|^3J(PC) + {}^5J(PC)| = 6.4$ Hz, $CH_{3(o)}$).

Synthesis and Characterization of 13, *rac*-(prophos)PdCl$_2$, and (dppe)PdCl$_2$. 13. To a solution of (S_C)-**6** (1.5 g, 2.84 mmol) in 1,2-dichloroethane (30 mL) was added a solution of $AgClO_4$ (0.65 g, 3.13 mmol) in water (1 mL), and the mixture was stirred for 30 min. The resulting mixture was filtered through a layer of Celite to remove AgCl, and the yellow-orange organic layer was dried over anhydrous $MgSO_4$. To the dried solution was added 0.74 mL (3.4 mmol) of allyldiphenylphosphine (ADPP) via syringe, and the reaction mixture was stirred magnetically under nitrogen for 6 days at 75 °C. The solvent was removed under reduced pressure to give a gummy dark red residue. This material was chromatographed on a silica gel column (40−200 mesh) with dichloromethane/ethyl acetate (4:1) as eluant. This resulted in a black band (containing elemental palladium and organic impurities) at the top of the column and an orange-red band which moved with the solvent front. The orange-red eluate was collected and evaporated in vacuo, giving a foamy brown solid. Dissolution of the solid in CH_3CN followed by slow addition of diethyl ether yielded **13**, which was isolated by filtration and dried in vacuo. Red prisms (0.42 g): mp 230−232 °C. Anal. Calcd for $C_{56}H_{59}Cl_4P_4Pd_4$: C, 49.27; H, 4.15; Cl, 9.97. Found: C, 42.14; H,4.21; Cl, 10.02. ^{31}P{^{1}H} NMR (202.3 MHz, $CDCl_3$, 25 °C): δ 221.92 (d, ^2J(PP) = 7.9 Hz, 2P, bridging phosphide), 42.49 (d, ^2J(PP) = 7.9 Hz, 2P, chelating phosphine). ^{1}H NMR (499.8 MHz, $CDCl_3$, 25 °C): δ 7.0−8.41 (m, 30H, Ph), 4.71 (m, 2H, H_4), 4.12 (m, 2H, H_1), 2.84 (m, 2H, H_3), 2.44 (m, 4H, H_2), 1.85 (s, 6H, $CH_{3(b)}$), 1.11 (s, 6H, $CH_{3(c)}$), 0.59 (d, $^3J(CH_3H_3) = 7.0$ Hz, 6H, $CH_{3(a)}$).

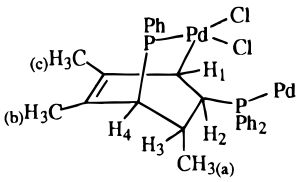

The remaining solution was then taken to dryness on a rotary evaporator to give a dark red oily residue that could not be characterized. To an acetone solution of the residue (80 mL) was added 4.5 mL of 10 M HCl, and the mixture was heated at reflux for 1 h. An orange-colored solution formed during this period. The solvents were removed under reduced pressure to give an orange-colored oily residue that could not be crystallized from a variety of solvents tried and could not be identified by NMR spectroscopy. To an aqueous solution of this residue was added 4 mL of 18 M NaOH. Addition of NaOH caused the precipitation of some elemental palladium, and the aqueous solution was extracted with dichloromethane. The chiral naphthylamine auxiliary (0.53 g, 93.8%) was recovered from the dichloromethane extract after removing the solvent under reduced pressure.

***rac*-(prophos)PdCl$_2$ and (dppe)PdCl$_2$.** A mixture containing 1.5 g (2.84 mmol) of (S_C)-**6** and 0.74 mL (3.4 mmol) of ADPP in 30 mL of 1,2-dichloroethane was heated at 75 °C for 6 days. The solvent was then removed under reduced pressure to give a gummy yellow-brown residue. Dissolution of the residue in acetone followed by slow addition of diethyl ether afforded a colorless solid that was isolated by filtration. The resulting solid was recrystallized from a CH_2Cl_2/MeOH/ether mixture to give colorless prisms (0.46 g), which were shown by ^{31}P{^{1}H} NMR spectroscopy to be a 2.25:1 mixture of *rac*-(prophos)PdCl$_2$ and (dppe)PdCl$_2$, respectively, as illustrated in Scheme 4.

The chiral naphthylamine auxiliary (0.45 g, 92%) was recovered from the residue by sequential HCl and NaOH additions as described above.

***rac*-(prophos)PdCl$_2$.**[26] ^{31}P{^{1}H} NMR (202.3 MHz, CD_3NO_2, 25 °C): δ 66.50 (d, ^2J(PP) = 6.3 Hz, 1P, P_b), 48.22 (d, ^2J(PP) = 6.3 Hz, 1P, P_a). ^{1}H NMR (499.8 MHz, CD_3NO_2, 25 °C): δ 7.5−8.0 (m, 20H, Ph), 3.13 (tdq, $^2J(P_bH_1) = {}^3J(P_aH_1) = 12.0$ Hz, $^3J(H_1H_3) = 11.5$ Hz, $^3J(H_cCH_3) = 7.0$ Hz, 1H, H_1), 2.87 (dddd, $^3J(P_bH_2) = 47.0$ Hz, $^2J(H_2H_3) = 15.0$ Hz, $^2J(P_aH_2) = 11.0$ Hz, 1H, H_2), 2.50 (dddd, $^3J(P_aH_3) = 19.5$ Hz, $^2J(H_2H_3) = 15.0$ Hz, $^3J(H_1H_3) = 11.5$ Hz, 1H, H_3), 1.13 (dd, $^3J(P_bCH_3) = 14.0$ Hz, $^3J(CH_3H_1) = 7.0$ Hz, 3H, CH_3). The couplings were confirmed

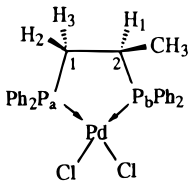

by COSY-45, ^{1}H {^{1}H sel}, and ^{1}H {^{31}P sel} experiments. ^{13}C{^{1}H} NMR (125.7 MHz, CD_3NO_2, 25 °C): δ 136.10 (d, ^2J(PC) = 11.2 Hz, C_o), 134.01 (d, ^2J(PC) = 11.3 Hz, C_o), 133.44 (d, ^2J(PC) = 10.4 Hz, C_o), 133.36 (d, ^2J(PC) = 8.5 Hz, C_o), 132.7 (d, ^4J(PC) = 2.6 Hz, C_p), 132.37 (d, ^4J(PC) = 3.1 Hz, C_p), 132.10 (d, ^4J(PC) = 3.1 Hz, C_p), 132.00 (d, ^4J(PC) = 3.0 Hz, C_p), 129.50 (d, ^1J(PC) = 56.3 Hz, C_i), 129.10 (d, ^3J(PC) = 11.8 Hz, C_m), 128.97 (d, ^3J(PC) = 11.8 Hz, C_m), 128.77 (d, ^3J(PC) = 10.8 Hz, C_m), 128.67 (d, ^3J(PC) = 11.7 Hz, C_m), 127.85 (d, ^1J(PC) = 54.2 Hz, C_i), 127.22 (d, ^1J(PC) = 53.7 Hz, C_i), 125.2 (d, ^1J(PC) = 51.7 Hz, C_i), 35.36 (dd, ^1J(PC) = 35.3 Hz, ^2J(PC) = 16.7 Hz, C_1), 35.17 (dd, ^1J(PC) = 32.9 Hz, ^2J(PC) = 13.4 Hz, C_2), 14.44 (dd, ^2J(PC) = 18.0 Hz, ^3J(PC) = 3.6 Hz, CH_3). Assignments were aided by APT and ^{13}C/^{1}H HETCOR experiments.

(dppe)PdCl$_2$.[25] ^{31}P{^{1}H} NMR (202.3 MHz, CD_3NO_2, 25 °C): δ 59.69 (s). ^{1}H NMR (499.8 MHz, CD_3NO_2, 25 °C): δ 7.5−8.0 (m, 20H, Ph), 2.70 (m, ([A_2X]$_2$, 4H, CH_2). ^{13}C {^{1}H} NMR (125.7 MHz, CD_3NO_2, 25 °C): δ 133.65 (AXX′, $|^2J(PC) + {}^4J(PC)|$ = 11.3 Hz, C_o), 132.26 (s, C_p), 128.93 (AXX′, $|^3J(PC) + {}^5J(PC)|$ = 8.3 Hz, C_m), 128.23 (dd, ^1J(PC) = 56.4 Hz, ^2J(PC) = 2.4 Hz, C_i), 28.30 (AXX′, $|^1J(PC) + {}^2J(PC)|$ = 48.1 Hz, CH_2).

C. X-ray Data Collection and Processing. Crystals of **1b**, **1c**, and **2b** were obtained by slow diffusion of hexane into a saturated CH_2Cl_2 solution of each compound. Pale yellow prisms of **2a** were obtained from a hot benzene solution. Pale yellow prisms of **5** were grown by slow diffusion of a 1:1 mixture of hexanes−ether into a saturated CH_2Cl_2 solution. Pale yellow prisms of **7** were obtained by slow diffusion of a 1:1 mixture of hexanes−ether into a saturated $CHCl_3$−acetone solution. Colorless crystals of **8**, **10**, and **11a** were obtained by slow diffusion of ether into a saturated CH_3CN−acetone solution of each compound. Crystals of **9**, **9a**, and **12** were grown by slow diffusion of ether into a saturated acetone solution of each compound. Red prisms of **13** were obtained by slow diffusion of ether into a saturated CH_3CN solution.

A suitable crystal of each compound was mounted on a glass fiber coated with epoxy and placed on a Siemens P4 diffractometer. Intensity data were taken in the ω mode at 298 K with Mo Kα graphite-monochromated radiation (λ = 0.71073 Å). Three check reflections, monitored every 100 reflections, showed random (<2%) variation during the data collections. The data were corrected for Lorentz and polarization effects and absorption (using an empirical model derived from azimuthal data collections, except for **13**, for which XABS[29] was used). Scattering factors and corrections for anomalous dispersion were taken from a standard source.[30] Calculations were performed with the Siemens SHELXTL PLUS (versions 5.03 or 5.10) software package on a personal computer. The structures were solved by direct (**5**, **6**, **7**, **8**, **9**, **9a**, **10**, **11a**, **13**) or Patterson (**1b**, **1c**, **2a**, **2b**, **12**) methods. Anisotropic thermal parameters were assigned to all non-hydrogen atoms. Hydrogen atoms were refined at calculated positions with a riding model in which the C−H vector was fixed at 0.96 Å. The data were refined by the method of full-matrix least-squares on F^2. Absolute configurations were determined by refinements of the Flack parameter[31] and were aided by the known configuration of the carbon stereocenter.

Acknowledgment. This research was supported by an award from the Research Corporation, for which we are grateful. We thank Professor David A. Lightner for his generous permission to use the polarimeter. We are grateful to the National Science Foundation (Grant No. CHE-9214294) for funds to purchase the 500 MHz NMR spectrometer.

Supporting Information Available: Structural drawings of **1c**, **2a**, **7**, and **11a**, additional ^{1}H and ^{13}C{^{1}H} NMR data for **1a**, **1b**, **1c**, **2a**, **2b**, and **2c**, and tables of X-ray crystallographic data, atomic coordinates, hydrogen atom coordinates, anisotropic thermal parameters, and interatomic distances and angles for **1b, 1c, 2a**, **2b**, **5, 7**, **8, 9**, **9a**, **10**, **11a**, **12**, and **13**. This material is available free of charge via the Internet at http://pubs.acs.org.

OM990681A

(29) Parkins, S.; Moezzi, B.; Hope, H. XABS2: An emperical absorption corrections program. *J. Appl. Crystallogr.* **1995**, 53−56.
(30) *International Tables for X-ray Crystallography*; D. Reidell Publishing Co.: Boston, 1992; Vol. C.
(31) Flack, H. D. *Acta Crystallogr.* **1983**, *A39*, 876.